Security Classification

AD 744950

DOCUMENT CONTROL DATA - R&D

(Security classification of title, body of abstract and indexing annotation must be entered when the overall report is classified)

1. ORIGINATING ACTIVITY (Corporate author) NAVAL AIR PROPULSION TEST CENTER (AE) NAVAL BASE PHILA., PA. 19112	2a. REPORT SECURITY CLASSIFICATION UNCLASSIFIED 2b. GROUP

3. REPORT TITLE

Rotor Burst Protection Program - Phases VI and VII: Exploratory Experimentation to Provide Data for the Design of Rotor Burst Fragment Containment Rings

4. DESCRIPTIVE NOTES (Type of report and inclusive dates)

Phase Report

5. AUTHOR(S) (Last name, first name, initial)

6. REPORT DATE	7a. TOTAL NO. OF PAGES	7b. NO. OF REFS
March 1972		

8a. CONTRACT OR GRANT NO. b. PROJECT NO. NASA DPR C-41581-B and C-41581-B, Mod. 1 c. d.	9a. ORIGINATOR'S REPORT NUMBER(S) NAPTC-AED-1968 9b. OTHER REPORT NO(S) (Any other numbers that may be assigned this report)

10. AVAILABILITY/LIMITATION NOTICES

Distribution of this report is unlimited.

11. SUPPLEMENTARY NOTES	12. SPONSORING MILITARY ACTIVITY
	Department of the Navy Naval Air Systems Command

13. ABSTRACT

Presented are the results of exploratory experimentation that was conducted in NAPTC Rotor Spin Facility to provide criteria for the design of turbomachine rotor burst fragment containment rings. High-speed photography was used to study containment processes involving freely supported rings of different materials and a variety of rotor and flat disk fragments.

DD FORM 1 JAN 64 1473

UNCLASSIFIED
Security Classification

TABLE OF CONTENTS

LIST OF FIGURES

LIST OF FIGURES (CONT'D)

INTRODUCTION

1. This is the final report on Phases VI and VII of the Rotor Burst Protection Program (RBPP) which is being conducted by the Naval Air Propulsion Test Center (NAPTC) under the auspices of the National Aeronautics and Space Administration[1] (NASA).

2. The program was started when an investigation made by NAPTC for the NASA Committee on Aeronautical Systems[2] (reference a) revealed that commercial jet aircraft were experiencing uncontained engine rotor bursts[3] at a significant yearly rate. This investigation also disclosed that uncontained rotor bursts continued to occur at a relatively constant yearly rate even though other aircraft operational problems were responding favorably to the improvements and advancements being made in applicable technology. The persistence of the rotor burst problem seemed to indicate that an upper limit of rotor reliability had been reached; a limit not necessarily dictated by technology, but one that reflected the compromises in absolute reliability that are made in order to make commercial flight economically feasible. It appeared as though an irreducible number of rotor bursts would occur each year; Because of the catastrophic consequences that can be associated with such events, it was decided that positive methods of providing for passenger safety would have to be developed and employed to protect the passengers and vulnerable parts of the aircraft from the lethal and devastating high energy fragments that are generated by an uncontained rotor burst. In response to this decision to provide protection, the RBPP was established at NAPTC by NASA. The goal of this program is to develop and provide criteria for the design of flight-weight devices that can be used on jet powered aircraft to protect people and equipment from gas turbine engine rotor burst fragments.

3. Reports that document the development of this program and which present preliminary experimental results have been published by NAPTC; these are listed as references a, b, c and d.

4. This report presents the results of exploratory experiments that were conducted at NAPTC to provide information and data for the design of rotor fragment containment devices. It also contains an up-date of the statistics on the occurrence of jet engine rotor bursts in commercial aviation.

CONCLUSIONS

5. Regarding the rotor burst fragment containment process:

a. In a containment situation involving fragments from a typical axial flow turbomachine rotor, blade deformation constitutes almost all of the fragment

(1) Contract No. DPR C41581-B, Modifications 1 and 2.
(2) Formerly the NASA Advisory Committee on Aircraft Operating Problems.
(3) An uncontained rotor burst is defined as a rotor failure that produces fragments which penetrate and escape the confines of the engine casing.

deformation that occurs; the hub or disk portion of the fragment behaves as a rigid non-deformable body that causes distortion of the containment ring. The forces needed to deform the blades are relatively small, as are the energies absorbed by their deformation. Therefore, the blades on a rotor fragment do not significantly influence the distribution of the impact loads that are induced in a ring (provided the ring thickness approaches that required to effect containment and the fragment hub to blades mass ratio is large), nor do the blades absorb significant amounts of energy through their deformation during the containment process. The blades serve only to influence the fragment trajectory during the initial stages of impact. This also means that in cases where the rotor tip-to-ring clearance is small (test or operational clearances) the blade radial length becomes in effect the radial clearance that influences the orientation of the hub or disk portion of the fragment..

b. The amount of blade deformation sustained by the rotor fragments during containment appears to be independent of the hardness of the containment ring material. At equivalent burst speeds soft and hard materials alike cause the same type and degree of blade deformation.

c. The general displacement and deformation characteristics of containment rings, optimally designed for weight reduction and subjected to rotor fragment attack, do not significantly vary for rings made from materials having a wide range of strengths and ductilities. The ring distorts to conform to the shape of the undeformed disk portion of the rotor fragment. The number of ring distortion sites is equal to twice the number of fragments attacking the containment ring. The magnitude of ring distortion, and the time it takes for these distortions to develop depends on the ring mass, material strength, thickness or stiffness, and the speed of the fragments at impact.

d. The variables that appear to affect the containment processs most significantly are:

(1) The burst speed
(2) The number of fragments
(3) The blade tip-to-hub diameter ratio of the rotor fragments
(4) The ring length-to-thickness ratio
(5) The ring diameter
(6) The ring material

6. Regarding Rotor Burst Fragment Deflection:

Rotor fragments can be effectively deflected (their trajectories controlled) through the use of partial rings of reasonable weight.

7. Regarding the problem of jet engine rotor bursts in commercial aviation:

The rate of rotor bursts increased to approximately 31 bursts per year for the years 1969 and 1970. Because of the potentially catastrophic consequences of such events, this level of incidence of rotor bursts is considered high.

RECOMMENDATIONS

8. The program of systematic rotor burst containment experimentation outlined in Appendix A and now being conducted at the NAPTC should be continued to completion. This program was developed to provide data for the design of optimum weight rings that will contain the fragments from various size axial flow turbomachine rotors that burst at or near their operating design speed.

9. Experimental and analytical efforts to investigate the concept of partial shielding, or more aptly, rotor burst fragment deflection, should continue. Systematic approaches are being developed at NAPTC to experimentally produce criteria for the design of optimum weight rotor fragment deflection devices that will provide regions of protection from fragment attack.

DESCRIPTION OF EXPERIMENTS AND DISCUSSION OF RESULTS

10. Table I lists the rotor, disk and blade burst containment experiments that were conducted during Phases VI, and VII and part of VIII of the RBPP; it also briefly describes the hardware, materials and conditions involved in each experiment. These experiments were considered exploratory because they were conducted to learn something about the nature of the rotor burst containment process and to establish what variables significantly influence or characterize the dynamics and deformations involved in rotor burst containment. Because of their variety, the best way to describe the experiments conducted and discuss their results is to group and present them according to their objectives.

EVALUATION OF CONTAINMENT RING MATERIALS AND ROTOR FRAGMENT BEHAVIOR

11. These experiments involved subjecting rings of equal weight, but made from different materials having varied mechanical properties, to turbine rotor fragment attack. The objectives were to:

a. Determine what effect differences in material mechanical properties had on the characteristics of fragment and ring deformation.

b. Comparatively evaluate the fragment containment capabilities of the various materials used.

c. Evaluate a fragment containment ring design concept commonly called the strain energy method that enjoys widespread use in industry. This concept is expressed in equation form:

$$(1)\ W_R = \frac{KE_B}{\frac{1}{\rho}\int_0^{\varepsilon_f} f(\sigma,\ \varepsilon)}$$

Which in stated form says, that the weight of a ring (W_R) needed to contain rotor burst fragments can be estimated by dividing the total fragment energy (rotor energy at burst KE_B) by the area under the engineering stress-strain curve $\frac{1}{\rho}\int_0^{\epsilon_f} f(\sigma, \epsilon)$ for the ring material used, where ρ = ring material density

ϵ_f = ultimate strain, $f(\sigma, \epsilon)$ = function of engineering stress and strain.

12. For these experiments GE T58 engine power turbine rotors modified to burst into three equal pie sector fragments (as shown in Figure 1) were used as fragment generators. For each type of ring material studied, the burst speed and therefore the fragment attack energy was increased incrementally from experiment to experiment until ring failure occurred. The dynamics and deformation characteristics of the containment process involved in these experiments were recorded by high-speed photography. Figures 2 through 6, show selected frames from high-speed photographic sequences taken of 4130 steel, TRIP steel, 2024 (T_4) aluminum, ballistic nylon and filament wound E glass rings in the process of containing rotor burst fragments. These photographic results show that the gross ring and fragment deformations are approximately the same for all the ring materials tested. The rotor fragments experienced deformations involving only the blades which were curled and bent while the disk portion of the fragment remained intact and suffered no apparent deformation. Frame to frame analysis of the fragment displacements recorded by the high-speed photographs revealed that the time that it took blade deformations to occur was approximately the same regardless of the ring material used and varied only with burst speed. Blade deformation times became shorter as burst speed was increased.

The rings were displaced and deformed to generate the typical three lobed pattern associated with 3-fragment bursts; this is well illustrated in the high-speed photographs.

In all cases large displacements and deformations of the ring did not occur until fragment blade deformation was almost completed. This indicated that relatively small forces are generated by the blade deformation which occurs during the initial stages of containment. These results qualitatively confirm the results of single blade deformation analyses and experiments that were conducted by the Massachusetts Institute of Technology (MIT). The findings of the MIT investigation also indicated that the forces and energy needed to deform a blade, as it characteristically would during the containment process, were relatively small (approximately 500 in-lb of energy per blade). Based on these combined results some important observations can be made:

a. The rotor fragment blades in their deformation do not substantially absorb much of the fragment energy that must be dissipated during containment.

b. The blades by virtue of their length and mass distribution serve only to prescribe the location of the fragment center of mass and the radial distance through which the non-deformable hub mass must travel during the initial stages of containment. These factors influence the trajectory and orientation of the fragment during the latter stages of containment when pronounced ring displacements and stresses (deformations) are induced.

c. Because the blades deform so readily, radial clearance effects are minimized. Differences in rotor-to-casing radial clearances between experiment and actual turbomachine construction are small compared to the blade length. Therefore, the ring and fragment behavior observed during experiments using radial clearances as large as 0.5 inches would be representative of the behavior that could be expected in an engine where rotor-to-casing clearances are measured in thousandths of an inch.

13. A comparison of the fragment energy containment capability of the various rings tested is presented in Table II. The factor used to make this comparison is called the specific contained fragment energy (SCFE). This factor, which provides a measure of ring capability, is derived by dividing the fragment energy that was contained by the weight of the ring required to provide containment.

The comparison indicates that TRIP steel has the greatest containment capability of all the ring materials tested. However, it should be noted that these results are only indicative of the actual containment capabilities of the ring materials tested. During each of these experiments, the high-speed photographs revealed that the fragments were escaping the confines of the ring. The speed, or more aptly, the amount of residual energy with which a fragment escaped the ring depended on the deformation characteristics of the ring, which in turn was dependent on the mechanical properties of the ring material. Since materials having varied mechanical properties were used in these tests, it is logical to assume that the fragments escaped with varying amounts of residual energy depending on the ring material used. The prime objective of these experiments was to observe and record the fragment-ring interactions through the use of high-speed photography. To do this no obstructions could be placed at the ring ends to prevent axial escape of the fragments. The behavioral characteristics of both the fragments and ring materials have been well documented during this phase of exploratory experimentation; therefore, future tests made to evaluate the containment capabilities of various materials will be designed to prevent axial escape of the fragments.

14. Based on the analysis presented in paragraph 11.c. involving the area under the engineering stress-strain curve, the energy absorbing potential of a 7-lb. 4130 steel ring (having an axial length of $1\frac{1}{2}$ inches and an internal diameter of 15 inches) would be approximately 247800 in-lb. However, experimental results indicate that such a ring is capable of containing rotor fragments having three times this amount of energy. This indicates that containment ring design analyses based on this concept of strain energy tend to be too conservative and would not provide the optimum weight ring designs that are being sought for aircraft applications. The analysis is not sophisticated enough to take into account the many other mechanisms of energy dissipation such as heat, mechanical displacement, etc. that are associated with the rotor fragment containment process.

ROTOR BLADE CONTAINMENT:

15. In these experiments, blades from GE T58 engine power turbine rotors were modified to fail and impact containment rings made from 6061 (T_6) and 2024 (T_4) aluminum. These materials were selected because they were readily available and have mechanical properties that are well known at high rates of strain. Two types of rotor blade containment experiments of interest were conducted.

a. Single blade bursts in which one blade mounted on a rotor disk was modified to fail and produce a blade fragment.

b. Single blade bursts in which one blade in a fully bladed rotor was modified to fail.

16. These blade burst experiments were conducted to:

a. Study the blade and ring interactions and deformations during the containment process.

b. Record (by high-speed photography) and measure the ring displacements with respect to time. These motion data were to be used by MIT in their TEJ-2 computer program to obtain estimates of the force-time characteristics of the blade during the containment process. Reference e contains details of this TEJ-2 computer program.

c. The experiments in which one blade in a rotor was modified to fail were conducted to study the blade fragment and blade interactions and through comparison with isolated blade experiments determine what effect these interactions had on the containment process.

17. The results of representative blade-fragment containment experiments, which are in the form of high-speed photographs, are shown in Figures 7 and 8.

Figure 7 depicts the sequence of events that occur when an isolated blade is contained by a freely supported ring whose thickness is representative of an engine casing. The ring deformation is seen to be local and extensive. The blade was deformed in a curling manner characteristic of turbine blades. This is shown in the post test photograph of Figure 7. Figure 8 shows the sequence of events that occur when a blade from a rotor fails, impacts a casing, and interacts with the blades remaining on the rotor. Initially ring deformation resembles that produced by the isolated blade burst. This is reasonable because the rings used and the burst speeds are the same for each experiment. But as time progresses, increasing interaction of the blade fragment with the other blades is observed and a failure of the ring occurs. This comparison provides evidence that greater forces and energy transfers are induced by blade interaction and clearly indicates that the momentum imparted to the blade fragment by other blades in the rotor adds measurably to its destructive potential. This imparted energy or momentum must be considered in any design analysis for blade containment rings or engine casings.

FLAT DISKS

18. The use of flat disks as fragment generators was explored during the earlier phases of containment experimentation. It was thought that they might be employed at less expense to simulate turbomachine rotor fragments. However, after some experimentation it became apparent that they would not serve this purpose. The type of loading imposed on a ring by a flat disk fragment was far different than that of a bladed rotor fragment. This is shown in Figures 2, 9 and 10 which contain high-speed photo sequences from flat-disk and bladed-rotor containment experiments. Although flat disk fragments are not applicable as rotor fragment simulators, the results of several experiments, in which attempts were made to contain 3-fragment flat disk bursts at various speeds using aluminum and steel rings, are presented in Table III. These data would be useful for the design of flywheel fragment containment rings.

FRAGMENT NUMBER

19. Containment experiments were conducted in which GE T58 engine power turbine rotors were modified to generate 2, 3, 4 and 6 symmetrical pie-sector shaped rotor fragments. Rings made from 4130 steel and having the same size and weight were used as containment devices. These experiments were conducted to determine what effect the number of rotor fragments had on the containment capability of the ring, or from another perspective, what number of fragments constituted the worst type of fragment attack condition for a containment ring. The results of these experiments (high-speed photographs) are shown in Figures 11 thru 14. The rings deformed symmetrically to form twice as many lobes as there were number of fragments involved in the attack. Too few experiments were conducted to draw any conclusions as to what number of fragments represented the worst impact condition. However, this will be studied more extensively during the next phase of investigation.

ROTOR FRAGMENT DEFLECTION DEVICES

20. Protecting an aircraft from rotor fragment attack through the use of partial rings, which would serve to redirect fragment to less sensitive and vulnerable areas of the aircraft, is an attractive concept, since it promises considerable weight savings over complete ring systems which are designed to capture or contain the fragments. Two significant experiments have been conducted to examine the feasibility of this concept and to study the mechanics that are involved in the deflection process. For the first experiment (120), two half-rings of equal size and weight were installed around a GE T58 engine power turbine that was modified to burst in half (refer pretest photo in Figure 15). One half-ring was welded to a rigid mount at one end; the other end was free of any attachment (hinged section). The other half-ring was welded to rigid mounts at both ends (fixed). This arrangement made it possible to observe and evaluate the behavior of two different deflection ring configurations during one experiment.

The objectives of this experiment were to examine the feasibility of using a half-ring to control the trajectory of a rotor fragment and to establish what method of half-ring attachment would be most effective for fragment deflection purposes. Selected high-speed photographs taken during the experiment are presented in Figure 15. They show that the rotor fragments impacted the half-rings close to their points of attachment; this impact condition was considered to be the worst possible, and therefore, provided a rigorous test of how well the half-rings functioned as fragment deflection devices.

The fixed half-ring experienced failures near the points of attachment soon after impact. The fragment did not, as might be expected, enter the "protected region" as a result of these failures. Instead the fragment continued to interact with the freed ring section and moved along what could be considered a safe trajectory.

The "hinged" half-ring behaved as anticipated: A plastic hinge formed close to the attachment point at impact. The half-ring pivoted about this point, while it guided the fragment over its inner surface along a safe, controlled trajectory away from the protected region.

The mounts for both half-rings failed during the fragment interaction. The results of this experiment demonstrate conclusively that half-rings can be used to provide suitable fragment trajectory control or deflection. However, the "hinged" half-ring appeared to function more effectively. In addition, it represented a lower weight [illegible] less complex configuration. The second experiment (123) was similar to the first involving the same type of modified rotor and two steel half-rings. However, the half-rings were of different weight (one weighing approximately twice the other), and they were freely suspended rather than being fixed at one or both of their end points. The objective of this experiment was to determine if the inertia of a half-ring alone would provide the constraint needed to control the fragment trajectory. The half-ring weights were different to provide different inertial responses to impact. Selected high-speed photographs of this experiment are presented in Figure 16. They show that the fragments struck the half-rings at points considered to be optimal for the evaluation of their trajectory control capabilities.

The lighter or thinner of the two half-rings (both half-rings had the same internal diameter and axial length) deformed considerably during the impact process and offered almost negligible resistance to fragment translational motion. As a result the fragment moved with considerable energy into the region that was to be protected by the half-ring.

The heavier half-ring was also deformed during impact but not to the same extent as the thin half-ring. Fragment translational motion was somewhat arrested as a result of the interaction, but the course of the fragment was not controlled. Like the other fragment, it too moved into the region to be protected. The behavior of both the fragment and half-ring after deformation was like that associated with the elastic collision of stationary and moving masses; where the mass with the initial momentum becomes stationary and the stationary mass is accelerated as a result of that collision. The results of these experiments indicate that a detailed experimental study to determine the effect of the following variables on the fragment deflection process would yield data pertinent to the development of criteria for the design of optimum weight rotor fragment deflection devices:

a. Ring material.
b. The partial ring size: I.D., thickness, axial length and arc length.
c. The ring constraints.
d. The point at which the fragment impacts the ring relative to its point of constraint.

THE INCIDENCE OF UNCONTAINED ROTOR BURSTS

21. Figure 19 shows the yearly incidence of uncontained jet engine rotor bursts in commercial aviation for the past nine years (1962 to 1970). During the past two years (1969 and 1970) an increase (over double those experienced in 1968) to an average of 31 uncontained rotor burst per year has been realized. The threat that these occurrences present to the welfare of commercial air travelers is still a vital and major concern to those who are liable and responsible for their safety, as is evidenced by continued support of the Rotor Burst Protection Program.

METHODS OF EXPERIMENT

22. Equipment: The experiments were conducted in chamber 1 of the NAPTC Rotor Spin Facility which is shown in Figure 17. A detailed description of this facility and the rotor drive equipment and accessories used are contained in reference b.

23. Instrumentation: A high-speed photo-instrumentation system was used to acquire data on fragment and ring behavior during the containment process. Details concerning the operation and performance of this system and the techniques used to photograph the containment process are also presented in reference b.

24. Experimental Techniques and Procedures: In each of the experiments discussed, the rotors or blades were typically modified, as shown in Figure 1, to fracture and generate fragments of prescribed size and shape at a preselected rotational speed.

The modified rotors were suspended from the spindle of a vertical drive turbine that was mounted on the chamber lid. A "catcher" bushing was used to arrest and limit the radial motion of the drive spindle induced by rotor fragmentation.

The containment rings were freely supported by thin radial wires and positioned concentrically around the rotors. A typical experiment set-up is shown in Figure 18. The operational procedure for these experiments was to evacuate the chamber (to minimize the aerodynamic rotor drag, which reduces drive turbine power requirements) and then rotationally accelerate the rotor to its burst speed.

REFERENCES

Reference material notes in this report is as follows:

a. "Turbine Disk Burst Protection Study" Phase I Final Report on Problem Assignment NASA DPR #R-105 - NAEC-AEL-1793 on 31 March 1965

b. "Turbine Disk Burst Protection Study" Final Phase II-III Report on Problem Assignment NASA DPR #R105 - NAPTC-AEL-1848 of 28 Feb 1967

c. "Rotor Burst Protection Program Initial Test Results" Phase III Final Report on Problem Assignment NASA DPR #R-105 - NAPTC-AED-1869 of 5 Apr 1968

d. "Rotor Burst Protection Program " Phase V Final Report on Problem Assignment NASA DPR #R-105 - NAPTC-AED-1901 of May 1969

e. NASA CR-72801, ASRLTR154-2, Sept 1970, On the Interaction Forces and Responses of Structural Rings Subjected to Fragment Impact.

TABLE 1

EXPERIMENT DATA COMPILATION

EXPERIMENT NO.	TYPE OF EXPERIMENT	ROTOR/DISK TYPE	ROTOR/DISK MATERIAL	DIAMETER INCHES	NO. OF FRAGMENTS	BURST SPEED- RPM	BURST ENERGY IN-LBS	CONTAINMENT/CONTROL SYSTEM CONFIG-URATION	MATERIAL	I.D. INCHES	THICKNESS INCHES	AXIAL LENGTH - IN.	WEIGHT LBS.
35	RB (a)	Turb. Rotor (d)	A-286	14.00	3	21500	923350	Ring	HY-140	14.500	0.235	3.00	5.40
36	RB	Turb. Rotor	A-286	14.00	3	21600	932400	Composite Ring	GAGA (f)	14.414	0.328	3.00	3.62
37	RB	Turb. Rotor	A-286	14.00	3	21600	932500	Composite Ring	AVCO (g)	14.502	1.095	3.25	10.92
38	BB (b)	Turb. Rotor	A-286	14.00	3	15000	19455	Ring	1020 Stl.	14.500	0.135	2.00	3.20
39	BB	Turb. Rotor	A-286	14.00	3	20000	11520	Composite Ring	GAGA (f)	14.500	0.327	3.00	2.52
40	RB	Turb. Rotor	A-286	14.00	3	21200	898300	Ring	4130 Stl.	14.500	0.500	1.50	8.93
41	RB	Turb. Rotor	A-286	14.00	3	22000	967400	Ring	PHILCO/FORD (h)	14.500	0.306	3.00	11.78
42	RB	Turb. Rotor	A-286	14.00	3	15000	449700	Ring	PHILCO/FORD (h)	14.500	0.308	3.00	11.80
46	DB (c)	Flat Disk (o)	4130 Stl.	14.00	2	16750	373500	Composite Ring	GAGA (f)	14.500	1.218	3.25	10.83
47	BB	Turb. Rotor	A-286	14.00	1	15350	6703	Ring	6061-T6 Al	14.500	0.175	1.00	0.78
48	DB	Flat Disk	4130 Stl.	14.00	2	19500	506200	Composite Ring	SHEK-CLOTH (i)	15.000	1.563	1.50	9.46
[illegible]	BB	Turb. Rotor	A-286	14.00	1	15500	6924	Ring	6061-T6-Al	14.500	0.175	1.00	0.79
[illegible]	RB	Turb. Rotor	A-286	14.00	3	21000	881450	Ring	6061-T6-Al	14.500	1.375	1.00	6.44
[illegible]	DB	Flat Disk	4130 Stl.	14.00	3	19300	2093700	Ring	2024-T4-Al	15.250	3.625	1.34	2.05
[illegible]	DB	Flat Disk	4130 Stl.	14.00	3	14590	120813	Ring	2024-T4-Al	15.250	3.000	0.75	8.40
[illegible]	DB	Flat Disk	4130 Stl.	14.00	3	14620	260350	Composite Ring	AVCO (g)	14.993	3.600	1.53	9.11
[illegible]	DB	Flat Disk	4130 Stl.	14.00	3	10950	146150	Composite Ring	AVCO (g)	14.990	3.551	1.53	8.40
[illegible]	BB	Turb. Rotor	A-286	14.00	1	15140	6607	Ring	6061-T6-Al	14.500	0.175	1.00	0.82
5[illegible]	DB	Flat Disk	4130 Stl.	14.00	3	10440	307900	Ring	6061-T6-Al	14.500	1.375	1.00	6.59
57	BB	Turb. Rotor	A-286	14.00	1	14580	6130	Ring	6061-T6-Al	14.500	0.175	1.00	0.74
[illegible]8	DB	Flat Disk	4130 Stl.	14.00	3	2640	19365	Ring	FOAMALUM (j)	15.000	4.844	1.75	11.03
[illegible]	DB	Flat Disk	4130 Stl.	14.00	3	5420	51900	Ring	1025 Stl.	14.221	0.100	1.503	2.84
[illegible]0	DB	Flat Disk	4130 Stl.	14.00	3	3940	22500	Ring	FOAMALUM (j)	15.018	4.341	1.396	7.98
61	RB	Turb. Rotor	A-286	14.00	3	8250	145800	Ring	4130 Stl.	15.002	0.338	1.504	6.90

TABLE I (CONT'D)

EXPERIMENT DATA COMPILATION

EXPERIMENT NO.	TYPE OF EXPERIMENT	ROTOR/DISK TYPE	MATERIAL	DIAMETER INCHES	NO. OF FRAGMENTS	BURST SPEED-RPM	ENERGY IN-LBS	CONTAINMENT/CONTROL SYSTEM CONFIGURATION	MATERIAL	I.D. INCHES	THICKNESS INCHES	AXIAL LENGTH-IN.	WEIGHT LBS.
62	DB	Flat Disk	4130 Stl.	14.00	3	5900	183700	Ring	4130 Stl.	15.035	0.323	1.525	6.99
63	RB	Turb. Rotor	A-286	14.00	3	19500	816900	Ring	4130 Stl.	15.004	0.326	1.500	6.99
64	DB	Flat Disk	4130 Stl.	14.00	3	9070	467610	Ring	4130 Stl.	15.000	0.3395	1.503	7.0
65	RB	Turb. Rotor	A-286	14.00	3	15950	546950	Ring	4130 Stl.	15.014	0.335	1.494	6.97
66	DB	Flat Disk	4130 Stl.	14.00	3	8530	412700	Ring	4130 Stl.	15.016	0.334	1.498	6.96
67	RB	Turb. Rotor	A-286	14.00	3	18830	760800	Ring	4130 Stl.	15.000	0.339	1.501	6.99
68	DB	Flat Disk	4130 Stl.	14.00	3	8600	419250	Ring	4130 Stl.	15.005	0.339	1.505	7.02
69	RB	Turb. Rotor	A-286	14.00	3	20860	933950	Ring	4130 Stl.	15.006	0.332	1.504	7.04
70	DB	Flat Disk	4130 Stl.	14.00	3	5700	184440	Ring	4130 Stl.	15.003	0.341	1.501	7.00
71	RB	Turb. Rotor	A-286	14.00	3	20330	878300	Composite Ring	AVCO (g)	14.906	2.232	1.506	9.87
72	RB	Turb. Rotor	A-286	14.00	1	21600	13200	Ring	6061-T6 Al.	14.249	0.395	1.000	1.37
73	RB	Turb. Rotor	A-286	14.00	3	20220	878300	Composite Ring	AVCO (g)	14.225	1.909	1.523	7.30
74	RB	Turb. Rotor	A-286	14.00	3	20860	933950	Ring	2024-T3-Al.	15.000	0.930	1.505	7.08
75	RB	Turb. Rotor	A-286	14.00	3	14450	448000	Ring	2024-T3-Al.	15.000	0.929	1.513	7.13
76	RB	Turb. Rotor	A-286	14.00	3	14260	442100	Ring	FOAMALUM (j)	15.000	4.813	3.688	17.05
77	DB	Flat Disk	4130 Stl.	14.00	3	6660	251600	Ring	4130 Stl.	15.000	0.342	1.500	6.95
78	RB	Turb. Rotor	A-286	14.00	4	18180	685140	Ring	4130 Stl.	15.000	0.340	1.500	6.93
79	RB	Turb. Rotor	A-286	14.000	3	12890	356500	Ring	2024-T3-Al.	15.000	0.938	1.514	7.11
80	RB	Turb. Rotor	A-286	14.00	4	18520	696100	Ring	4130 Stl.	15.004	0.341	1.501	6.95
81	RB	Turb. Rotor	A-286	14.00	2	20920	944100	Ring	4130 Stl.	15.008	0.387	1.501	6.95
82	DB	Flat Disk	4130 Stl.	14.00	2	9780	399520	Partial Ring	1025 Stl.	15.000	0.390	1.500	3.95
83	RB	Turb. Rotor	A-286	14.00	3	8330	393100	Partial Ring	1020 Stl.	15.000	0.390	1.500	3.95
84	RB	Turb. Rotor	A-286	14.00	1	11510	13340	Ring	2024-T4-Al.	14.986	0.145	1.973	1.49
85	RB	Turb. Rotor	A-286	14.00	1	[illegible]	7050	Ring	2024-T4-Al.	14.986	0.145	1.973	1.49

TABLE I (CONT'D)

EXPERIMENT DATA COMPILATION

EXPERIMENT NO.	TYPE OF EXPERIMENT	TYPE	MATERIAL	DIAMETER INCHES	NO. OF FRAGMENTS	BURST SPEED-RPM	ENERGY IN-LBS	CONFIGURATION	MATERIAL	I.D. INCHES	THICKNESS INCHES	AXIAL LENGTH-IN.	WEIGHT LBS.
86	RB	Turb. Rotor	A-286	14.00	3	18160	707700	Composite Ring	E-Glass (k)	14.982	1.364	1.505	7.79
87	DB	Flat Disk	4130 Stl.	14.00	2	7730	293300	Partial Rings	1025 Stl.	15.000	0.375 0.750	1.500	[illegible] 7.83
88	BB	Turb. Rotor	A-286	14.00	1	15400	6810	Ring	2024-T4-Al	17.313	0.173	1.505	1.46
89	BB	Turb. Rotor	A-286	14.00	3	21240	37400	Concentric Rings	304 S.S.	15.004 22.004	0.0319 0.045	1.492	3.42
90	RB	Turb. Rotor	A-286	14.00	4	18220	716330	Ring	4130 Stl.	14.988	0.350	1.502	7.05
91	BB	Turb. Rotor	A-286	14.000	1	15650	7950	Ring	2024-T4-Al	17.314	0.176	1.506	1.46
92	RB	Turb. Rotor	A-286	14.00	4	19250	807360	Ring	4130 Stl.	15.002	0.332	1.501	6.92
93	RB	Turb. Rotor	A-286	14.00	3	18500	732500	Grooved Composite Ring	E-Glass (k)	16.000	0.854	1.504	5.92
94	RB	Turb. Rotor	A-286	14.00	3	20700	919200	Grooved Ring	4130 Stl.	15.002	0.1875	1.507	7.13
[illegible]	RB	Turb. Rotor	A-286	14.00	3	20600	910350	Ring	TRIP Stl.	15.051	0.325	1.5235	7.08
[illegible]	RB	Turb. Rotor	A-286	14.00	3	18425	728450	Ring	4130 Stl.	15.001	0.3432	1.502	6.99
[illegible]	RB	Turb. Rotor	A-286	14.00	3	18830	761600	Grooved Composite Ring	AVCO (g)	14.995	0.409	1.506	5.48
[illegible]	RB	Turb. Rotor	A-286	14.00	3	20630	913140	Grooved Ring	TRIP Stl.	15.234	0.303	1.503	6.67
[illegible]	DB	Flat Disk	4130 Stl.	14.00	3	8300	314080	Ring	4130 Stl.	15.001	0.343	1.500	7.04
[illegible]	RB	Turb. Rotor	A-286	14.00	3	20860	933950	Grooved Ring	TRIP Stl.	15.161	0.250	1.488	5.64
101	RB	Turb. Rotor	A-286	14.00	3	18030	697850	Grooved Ring	E-Glass (k)	15.500	1.101	1.500	6.85
102	RB	Turb. Rotor	A-286	14.00	3	18260	715550	Ring	4130 Stl.	15.001	0.168	3.025	7.03
103	RB	Turb. Rotor	A-286	14.00	3	17670	670050	Ring	4130 Stl.	15.001	0.511	0.992	6.98
104	RB	Turb. Rotor	A-286	14.00	3	16560	567700	Ring	4130 Stl.	15.011	0.162	3.031	6.95
[illegible]	RB	Turb. Rotor	A-286	14.00	3	12170	230230	Grooved Composite Ring	Boron/Carb Fiberglass (m)	15.010	0.447	1.467	5.61
[illegible]	RB	Turb. Rotor	A-286	14.00	3	18070	706830	Ring	4130 Stl.	16.802	0.339	1.351	6.98
107	RB	Turb. Rotor	A-286	14.00	3	20840	869200	Grooved Ring	TRIP Stl.	15.321	0.180	1.528	4.52
108	RB	Turb. Rotor	A-286	14.00	3	18920	767950	Ring	4130 Stl.	15.001	0.342	1.401	8.9
[illegible]	RB	Turb. Rotor	A-286	14.00	1	15250	6450	Ring	6061-T6-Al	11.999	0.156	1.508	1.10

TABLE I (CONT'D)

EXPERIMENT DATA COMPILATION

EXPERIMENT NO.	TYPE OF EXPERIMENT	ROTOR/DISK TYPE	MATERIAL	DIAMETER INCHES	NO. OF FRAGMENTS	BURST SPEED-RPM	BURST ENERGY [illegible]	CONTAINMENT/CONTROL SYSTEM CONFIGURATION	MATERIAL	I.D. INCHES	THICKNESS INCHES	AXIAL LENGTH-IN.	WEIGHT LBS.
110	RB	Turb. Rotor	A-286	14.00	3	12840	353500	Grooved Composite Ring	Boron/Car.(m) [illegible] Fiberglass	15.500	0.282	1.531	2.64
111	BB	Turb. Rotor	A-286	14.00	1	15870	6910	Ring	6061-T6-Al.	15.001	0.155	1.502	1.09
112	BB	Turb. Rotor	A-286	14.00	1	15700	6800	Ring	6061-T6-Al.	15.005	0.148	1.502	1.10
113	RB	Turb. Rotor	A-286	14.00	3	20250	880150	Grooved Ring	TRIP Stl.	15.172	0.249	1.498	5.52
114	BB	Turb. Rotor	A-286	14.00	1	15700	7120	Ring	6061-T6-Al.	15.002	0.150	1.502	1.09
115	RB	Turb. Rotor	A-286	14.00	3	13290	353200	Square	Strongskin(n) Panels	18.750	0.750 1.250	8.000	10.57
116	BB	Turb. Rotor(o)	D-979	18.53	1	14470	–	Grooved Ring	1020 Stl.	19.000	0.250	3.500	21.20
117	RB	Turb. Rotor	A-286	14.00	3	13780	407350	Grooved Composite Ring	Boron/Car. Fiberglass	15.000	0.687	1.502	4.49
118	RB	Turb. Rotor	A-286	14.00	3	11400	278150	Grooved Composite Ring	Boron/Car. Fiberglass	15.000	0.287	1.500	4.49
119	RB	Turb. Rotor	A-286	14.00	3	19640	825450	Ring	4130 Stl.	15.004	0.292	1.500	5.99
120	RB	Turb. Rotor	A-286	14.00	2	17830	679801	Partial Ring	4130 Stl.	15.000	0.294	1.500	–
121	RB	Turb. Rotor	A-286	14.00	3	18900	764100	Ring	4130 Stl.	15.002	0.342	1.500	7.03
122	RB	Turb. Rotor	A-286	14.00	3	18380	722800	Ring	4130 Stl.	15.003	0.341	1.500	6.91
123	RB	Turb. Rotor	A-286	14.00	2	18070	754000	Partial Ring	4130 Stl. 1020 Stl.	15.000 15.000	0.375 0.250	1.500	3.43 2.83
124	RB	Turb. Rotor	A-286	14.00	3	19720	909800	Ring	4130 Stl.	15.000	0.493	1.000	6.69

See page 16 for definition of notes (a) to (o)

NOTES FOR TABLE I:

a. Rotor Burst

b. Blade Burst

c. Disk Burst

d. Turbine Rotor GE T58 Engine, Axial Flow Power Turbine Rotor, Hub Ratio = 2.147 Blade Material: Sel

e. Turbine Rotor AVCO/Lycoming T55-L-11 Engine, Axial Flow Power Turbine Rotor, Hub Ratio = 1.871 Blade Material: 713C

f. Composite manufactured by Goodyear Aerospace Corp. comprised of ceramic, glasscloth, and nylon

g. Composite manufactured by AVCO Corporation comprised of steel and ballistic nylon

h. Dual Property Steel manufactured by Philco/Ford Corp.

i. Shok-Cloth, ballistic nylon cloth.

j. Aluminum foam manufactured by Foamalum Corporation

k. Composite ring manufactured by Eshbaugh Corp., Construction - E-glass roving, epoxy resin laminate

l. Trip Steel - Transformation Induced Plasticity Steel, manufactured by Philco/Ford Corporation

m. Composite ring manufactured by Reflective Laminates/Fansteel

n. Stresskin panels - manufactured by Stresskin Products Co. (2 panels 316L, 2 panels Inco 718)

o. Flat disk - Made from 4130 steel; 14 inch diameter; 3/8 inch thick.

TABLE II

RELATIVE MERITS OF MATERIALS

NO.	RING MATERIAL	WEIGHT LB.	DIMENSIONS - INCHES I.D.	TH'K.	A.L.	SCFE (1) IN - lb/LB
65	4130 Steel	6.97	15.016	0.335	1.494	78471
75	2024-T4 Alum.	6.95	15.000	0.929	1.512	64460 (2)
73	Ballistic Nylon	7.30	14.995	1.909	1.522	120316
95	Trip Steel	7.08	15.0514	0.3251	1.523	128581
86	Fil. Wound E-Glass	7.79	14.987	1.364	1.505	90845

(1) SCFE - Specific contained fragment energy (refer to paragraph 13)
(2) Not contained but listed to give relative merit of material.

TABLE III

CONTAINMENT CHARACTERISTICS FOR FLAT DISK BURSTS

NO.	BURST SPEED RPM	BURST ENERGY IN-LBS.	RING MATERIAL	WEIGHT LB.	DIMENSIONS-INCHES I.D.	TH'K.	A.L.	CONTAINMENT
70	5696	184437	4130 A Steel	7.0	15.003	0.341	1.501	C (1)
77	6656	251595	4130 A Steel	6.95	15.000	0.342	1.500	C
66	8525	412717	4130 A Steel	6.96	15.016	0.334	1.498	C
64	9074	467645	4130 A Steel	7.0	15.000	0.339	1.503	NC (2)
52	14585	1208129	2024-T4 Aluminum	8.40	15.250	2.000	0.750	C
59	5418	53907	1025 Steel	7.84	14.991	0.390	1.502	C

(1) Contained
(2) Not Contained

Note: Flat Disks made from 4130 Steel
Diameter: 14.0 Inches
Thickness. 0.375 Inches

TYPICAL ROTOR AND BLADE, MODIFIED TO FAIL AT PRESCRIBED ROTATIONAL SPEED PRODUCING FRAGMENTS OF DESIRED SHAPE, SIZE AND WEIGHT.

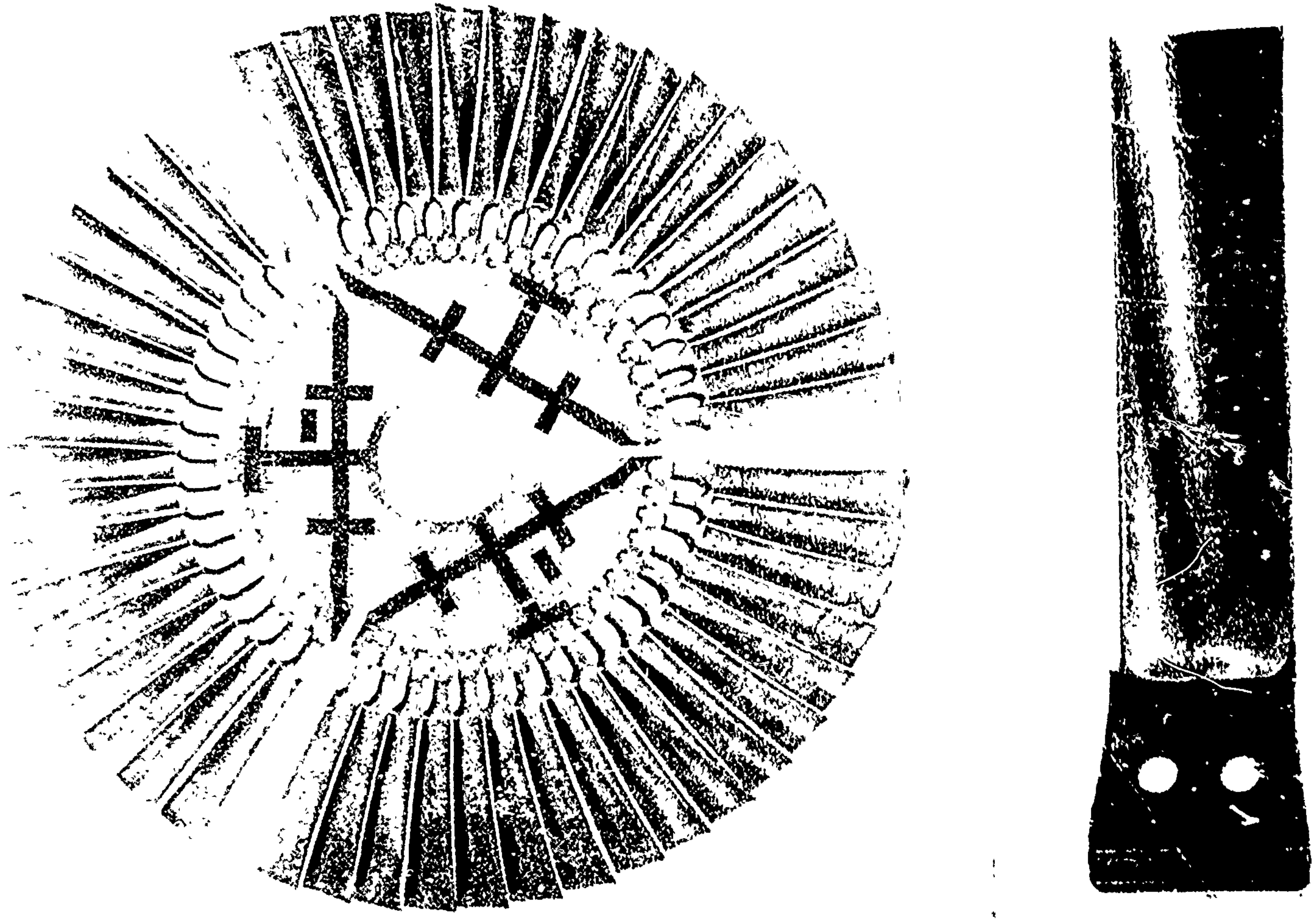

Figure 1

EXPERIMENT 67 -

3 FRAGMENT ROTOR BURST INTO A 4130 STEEL RING

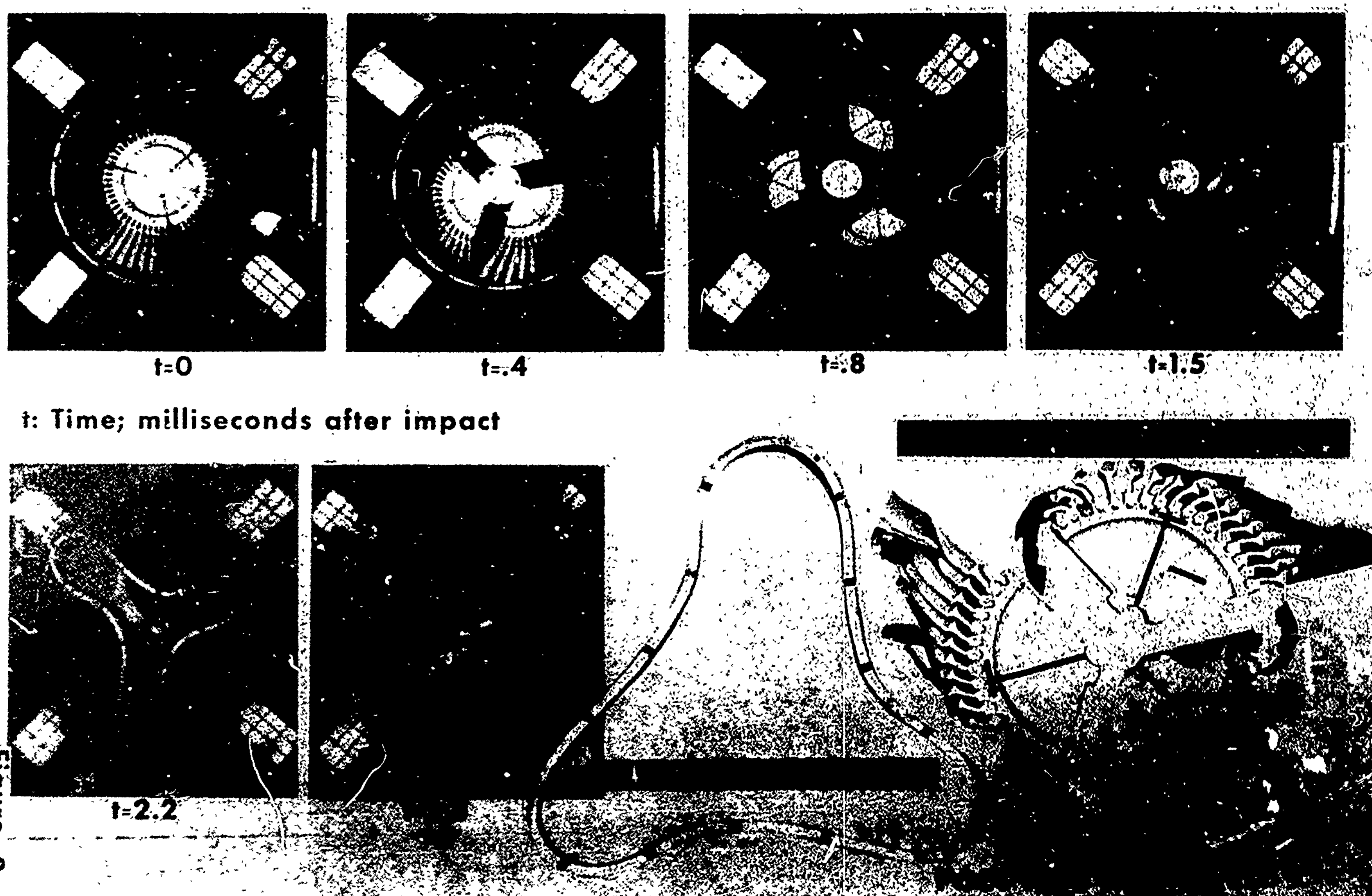

t: Time; milliseconds after impact

Figure 2

EXPERIMENT 100 -

3 FRAGMENT ROTOR BURST INTO A TRIP STEEL RING

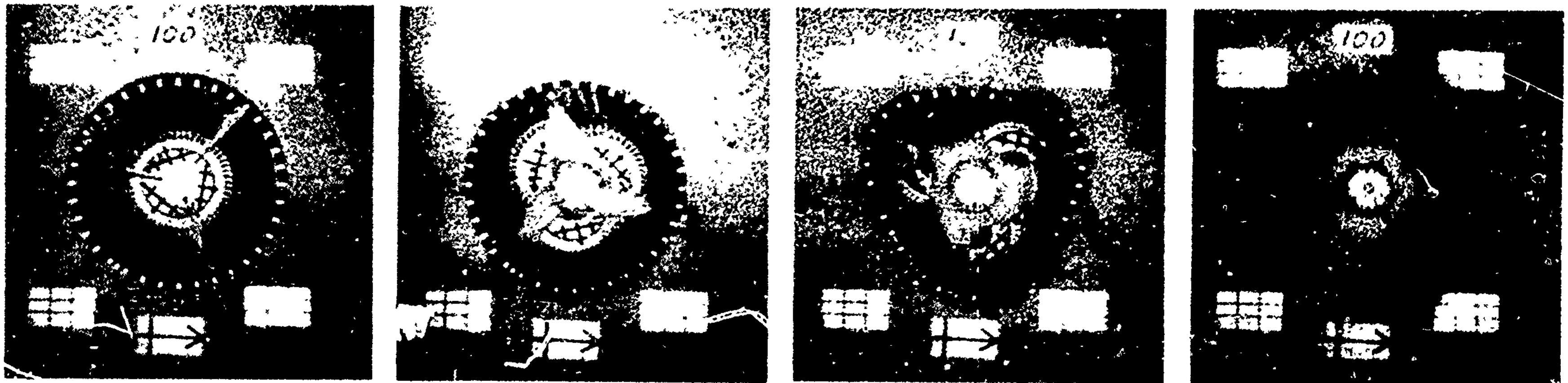

t=0 t=.4 t=.7 t=1.3

t: Time; milliseconds after impact

t=1.8 t=2.6

POST TEST

Figure 3

EXPERIMENT [illegible]4 -

3 FRAGMENT ROTOR BURST INTO A 2024-T4 ALUMINUM RING

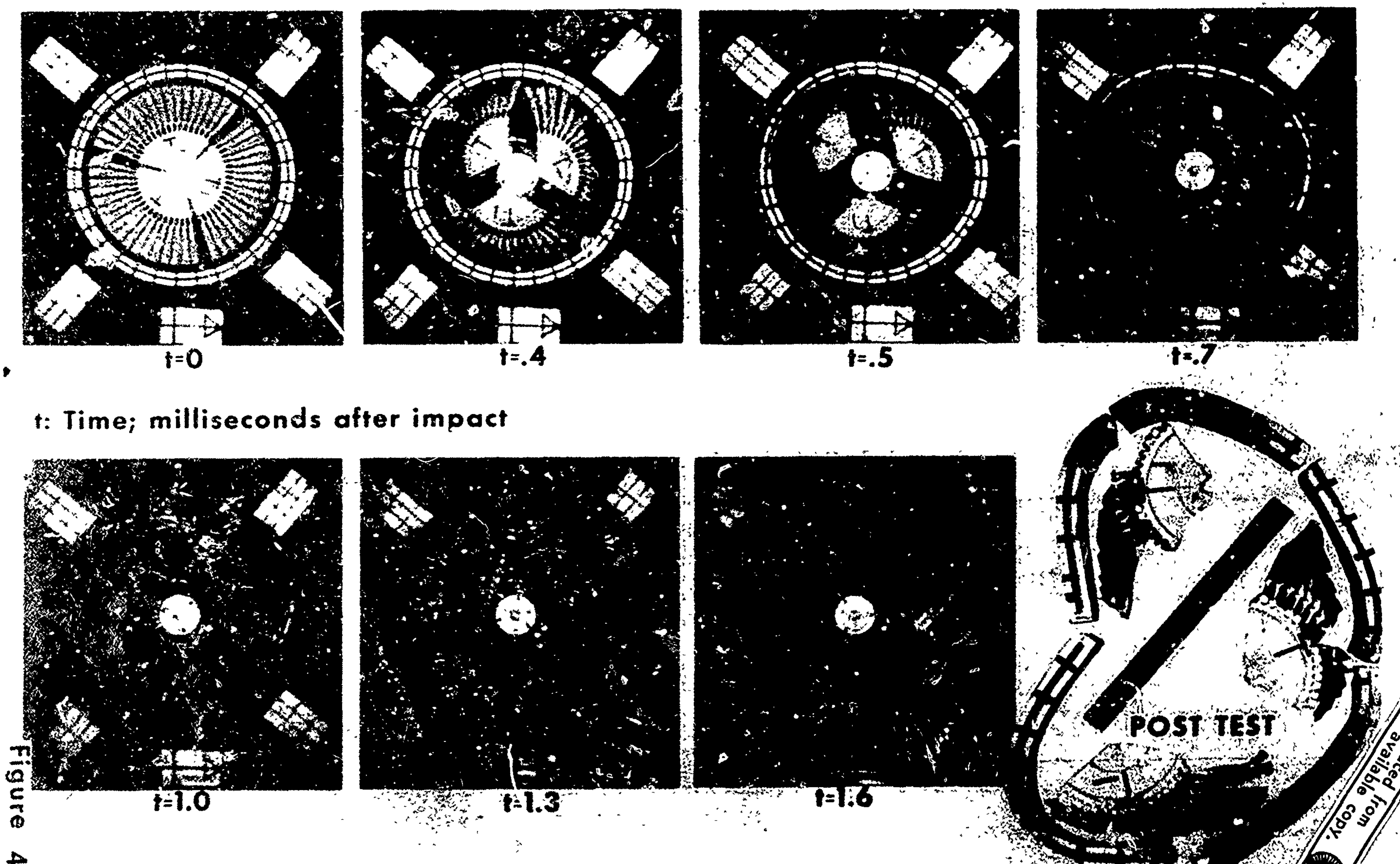

t: Time; milliseconds after impact

Figure 4

EXPERIMENT 71 -

3 FRAGMENT ROTOR BURST INTO A BALLISTIC NYLON WITH STEEL LINER RING

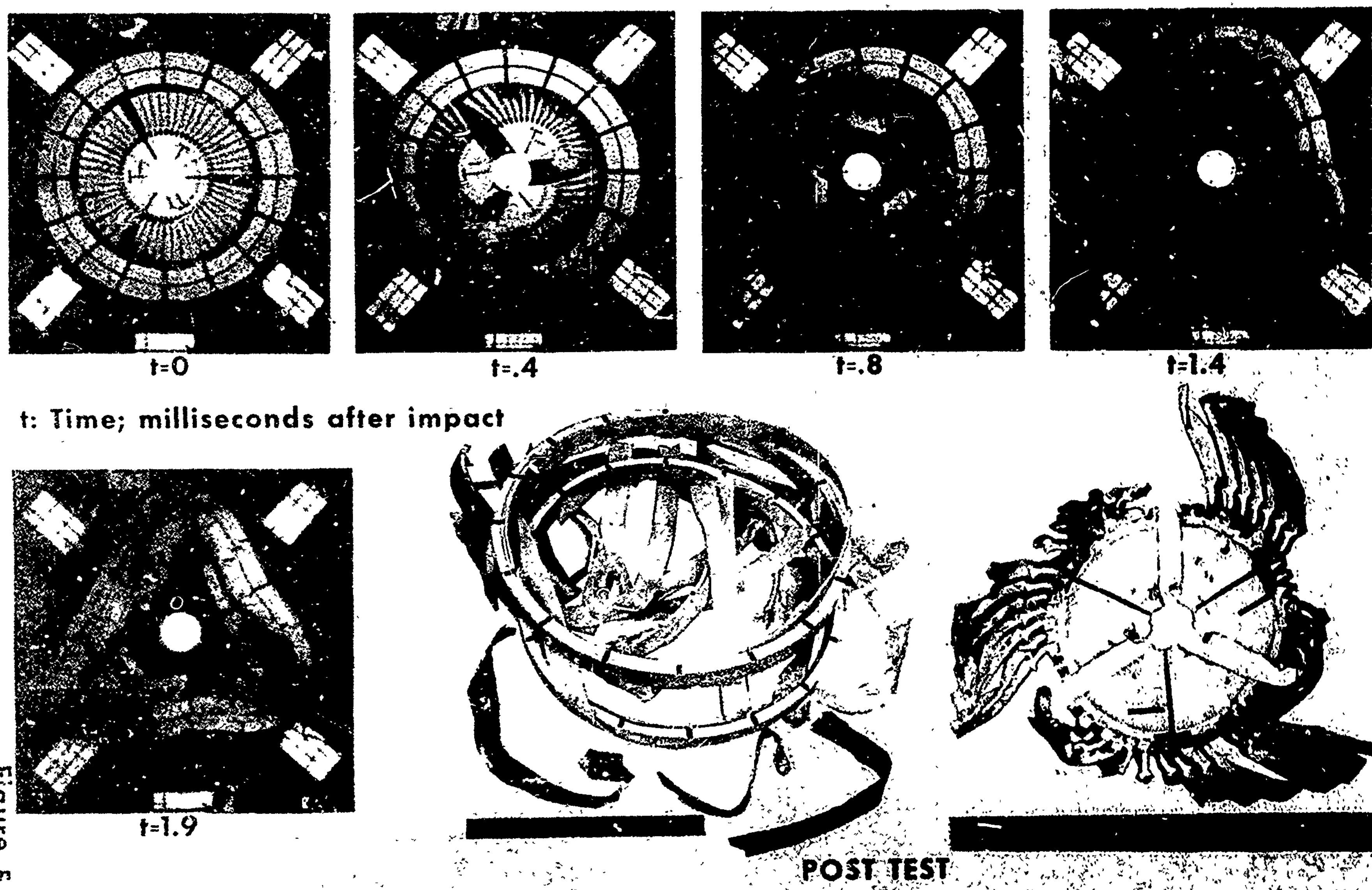

Figure 5

EXPERIMENT 86 -

3 FRAGMENT ROTOR BURST INTO A FILAMENT WOUND FIBERGLASS RING

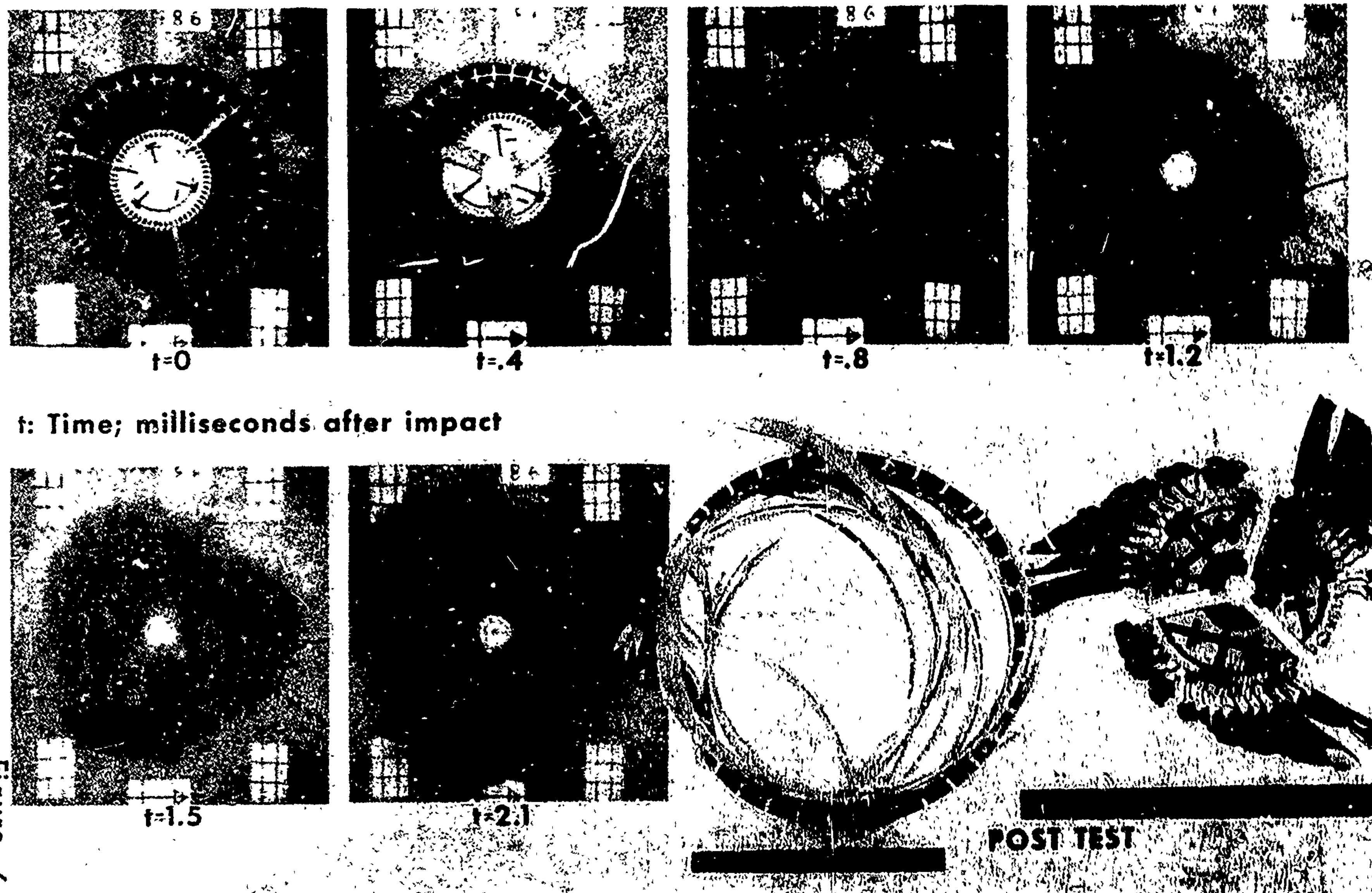

Figure 6

EXPERIMENT 109 -

SINGLE BLADE BURST INTO A 6061-T6 ALUMINUM RING

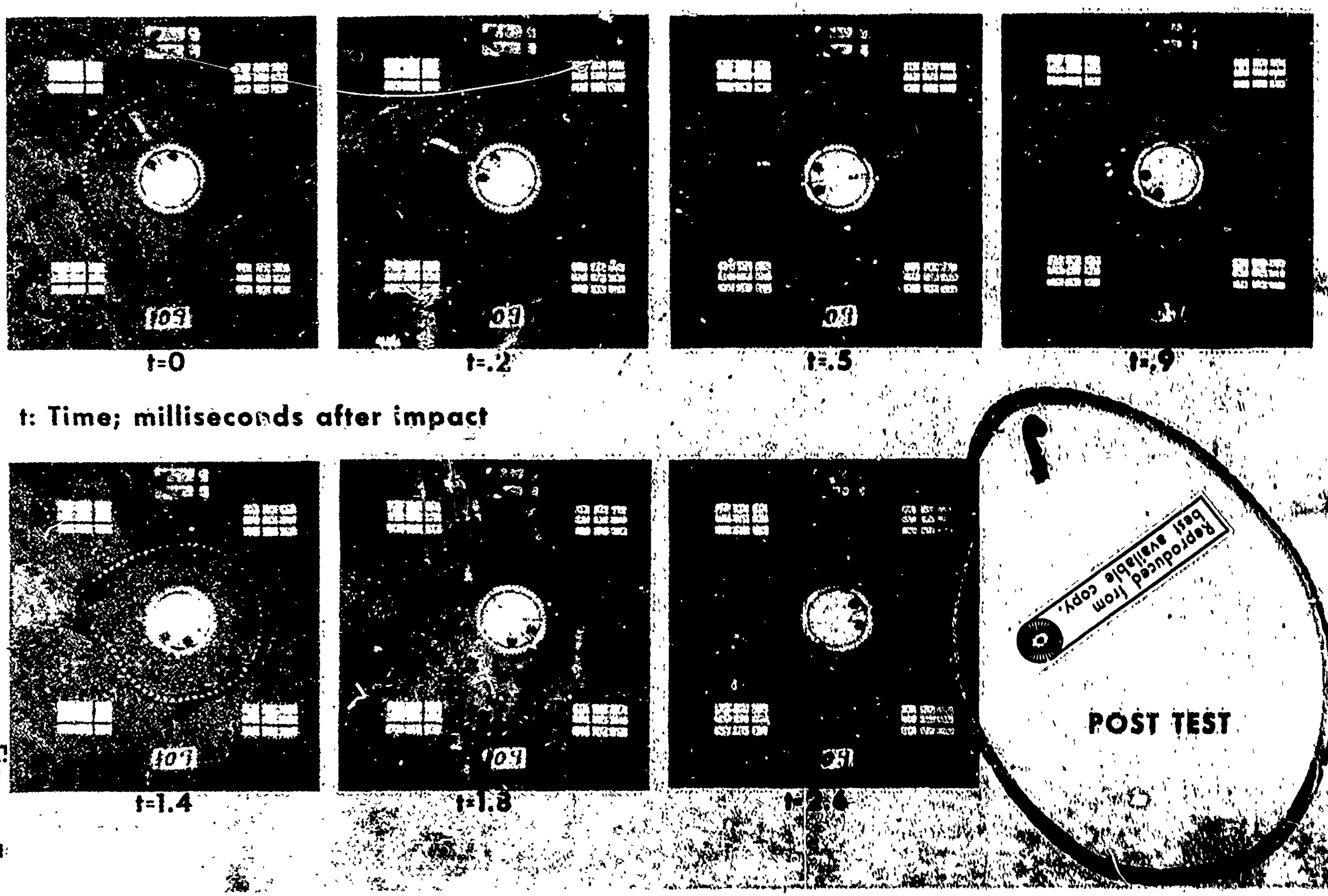

Figure 7

EXPERIMENT 114 -

ROTOR BLADE BURST INTO A 6061-T6 ALUMINUM RING

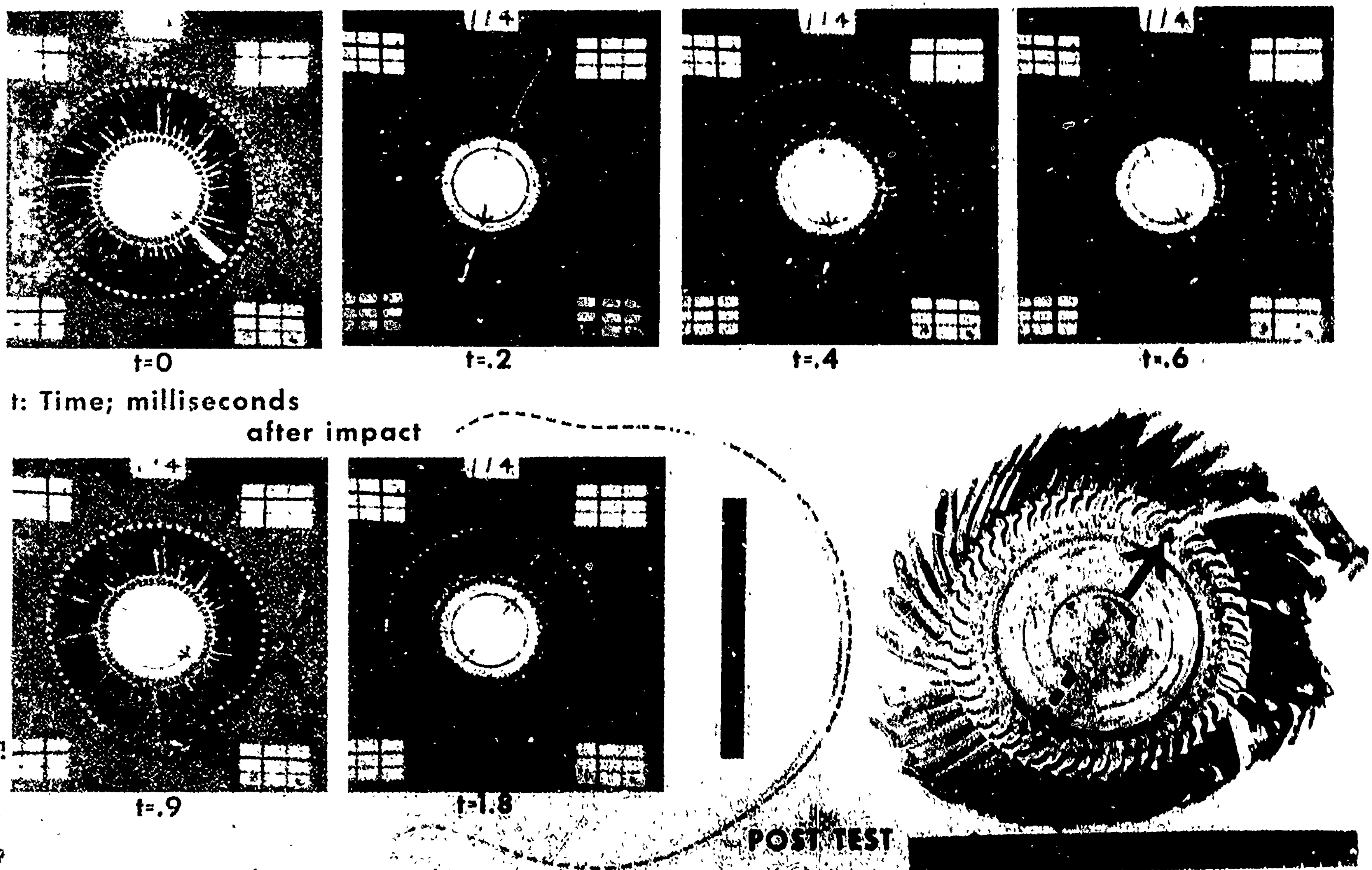

Figure 8

EXPERIMENT 64 -

3 FRAGMENT DISK BURST INTO A 4130 STEEL RING

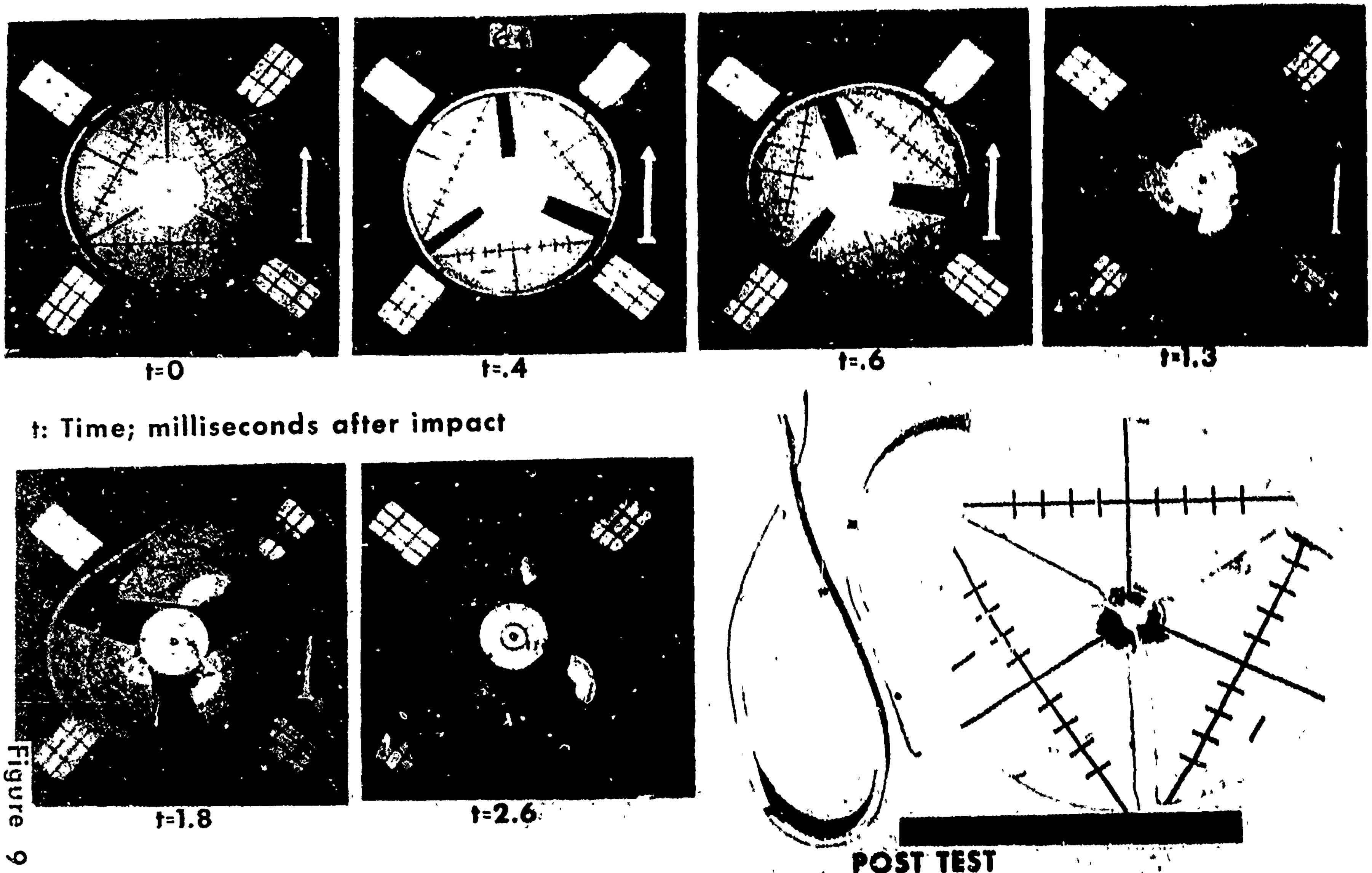

t: Time; milliseconds after impact

Figure 9

EXPERIMENT 52 -

3 FRAGMENT FLAT DISK INTO A 2024-T4 ALUMINUM RING

t: Time; milliseconds after impact

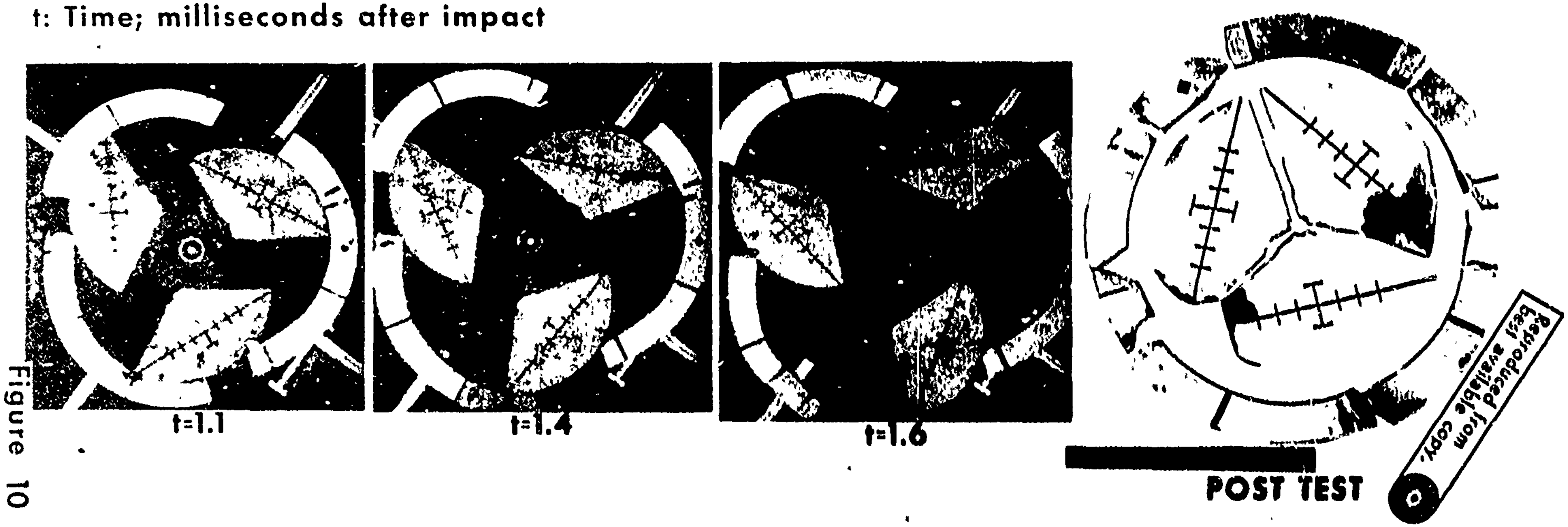

Figure 10

EXPERIMENT 81 -
2 FRAGMENT ROTOR BURST INTO A 4130 STEEL RING

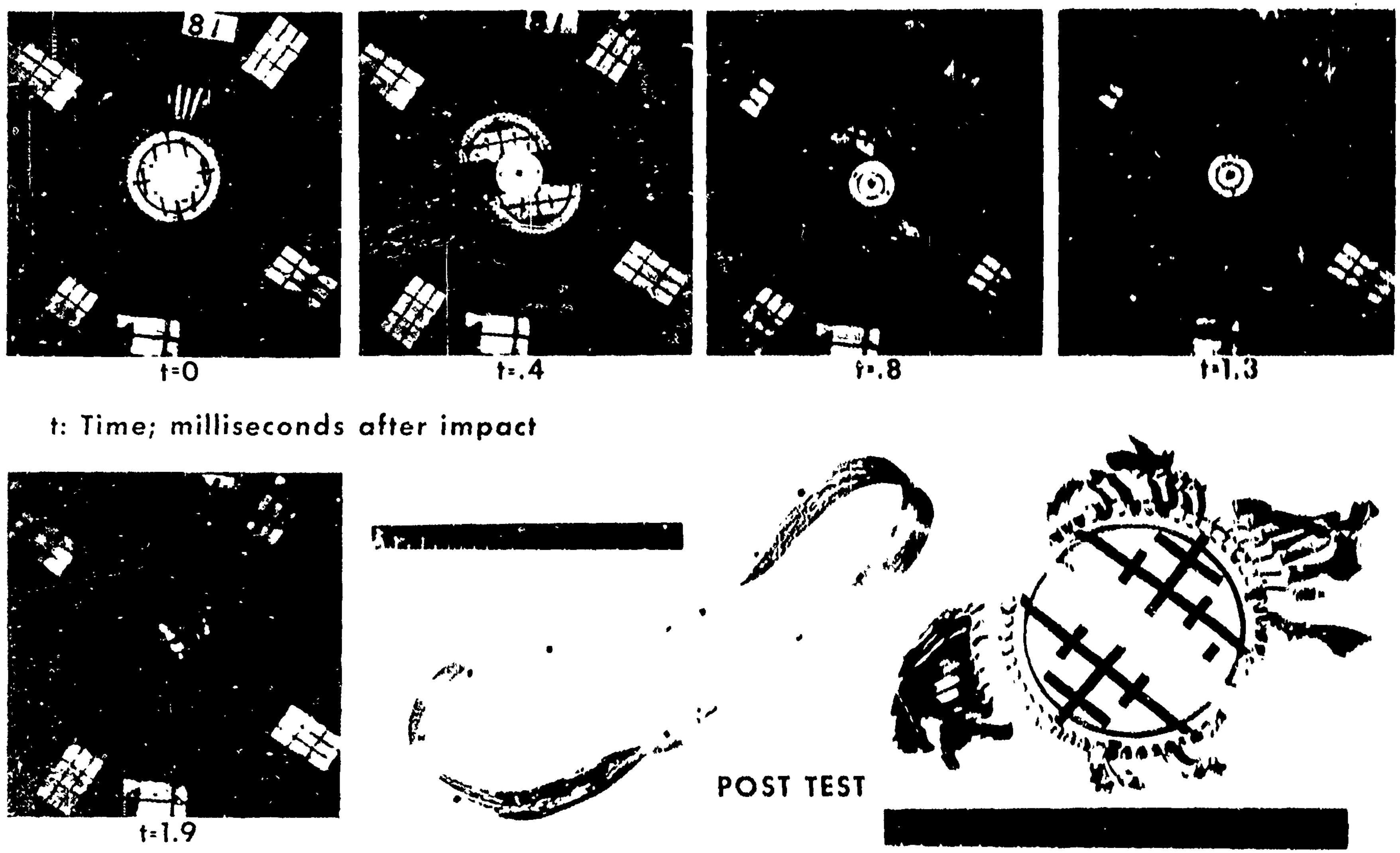

Figure 11

ᐟPERIMENT 65 -

3 FRAGMENT ROTOR BURST INTO A 4130 STEEL RING

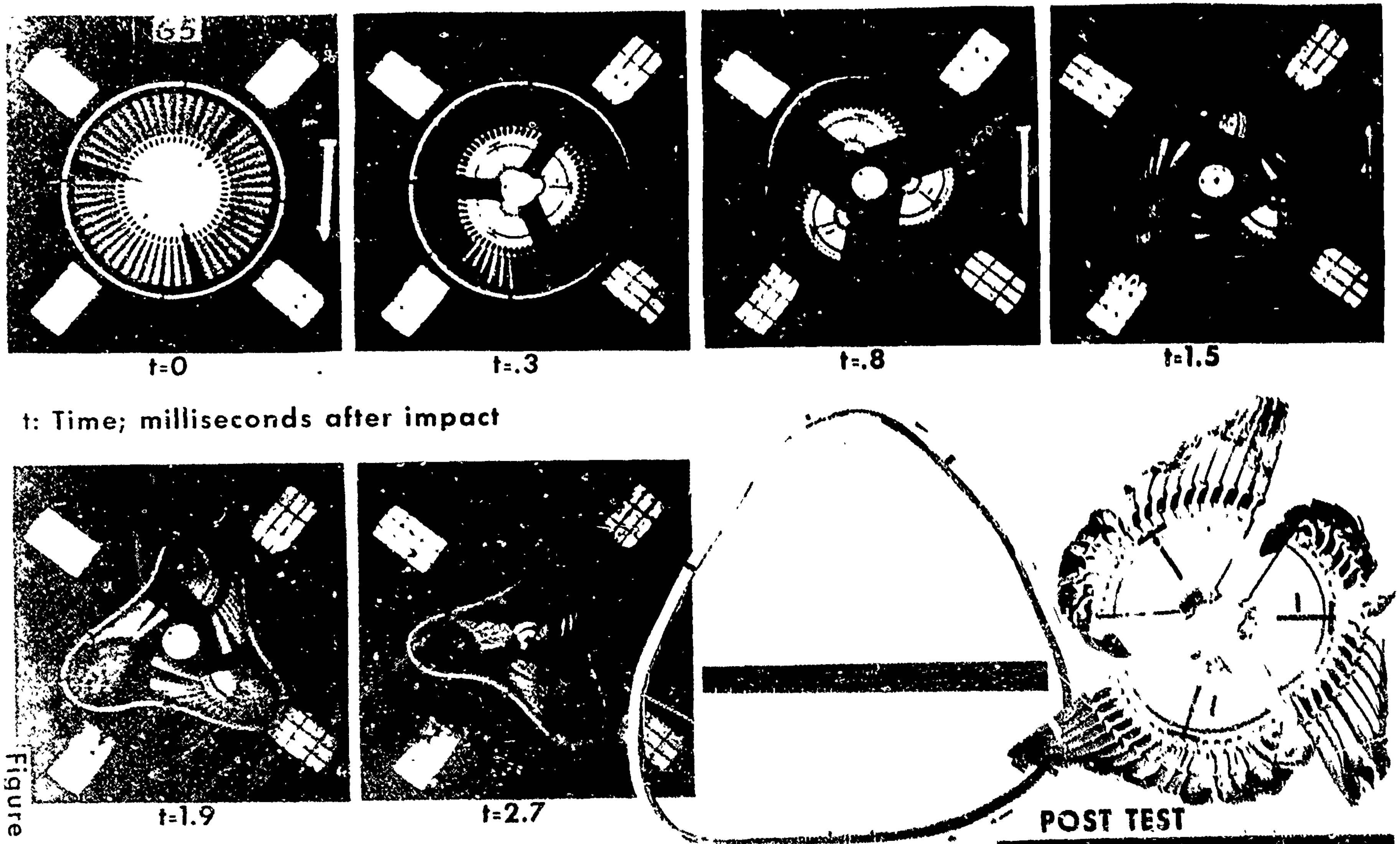

Figure 12

EXPERIMENT 90 -

4 FRAGMENT ROTOR BURST INTO A 4130 STEEL RING

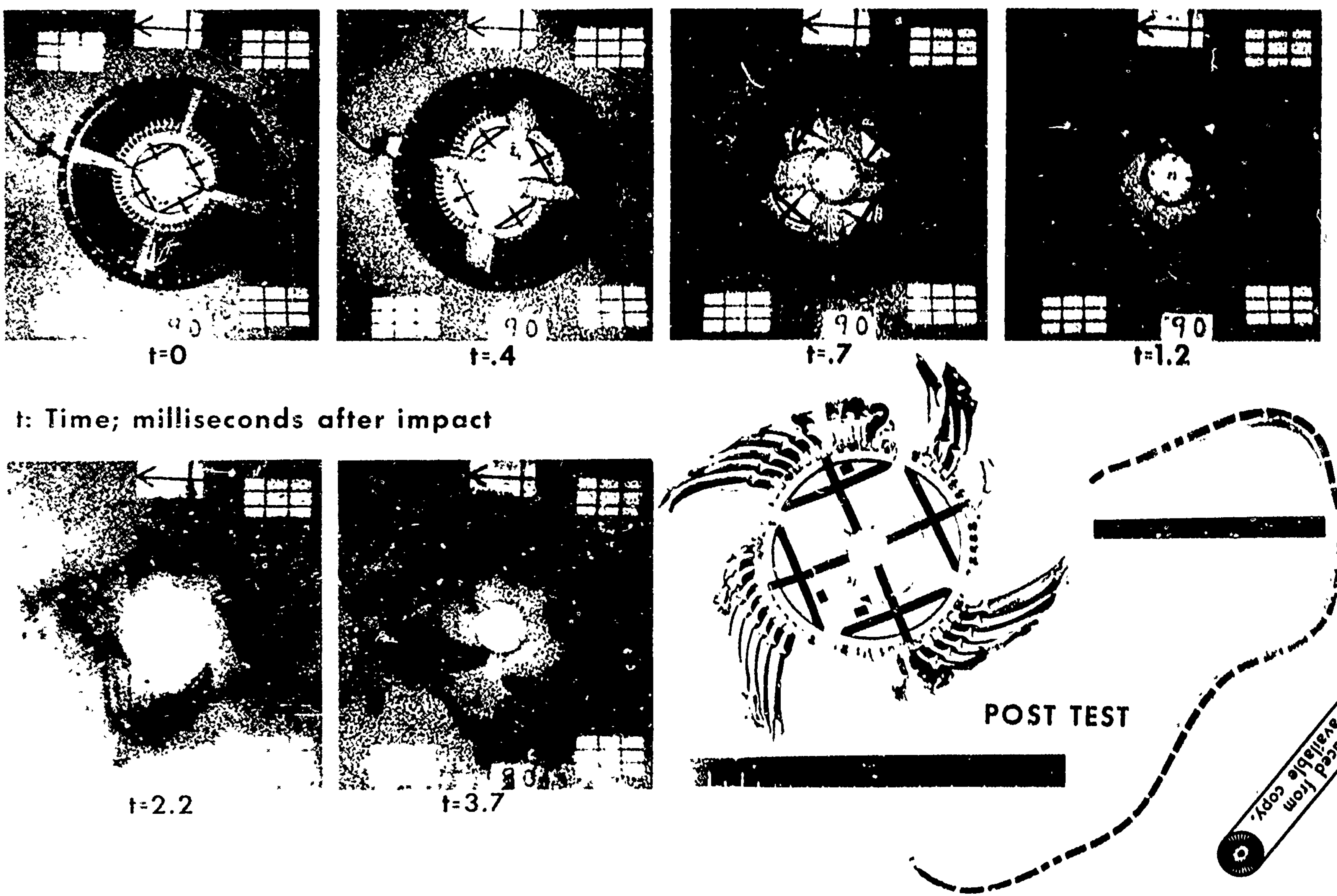

Figure 13

6 FRAGMENT ROTOR BURST INTO A 4130 STEEL RING

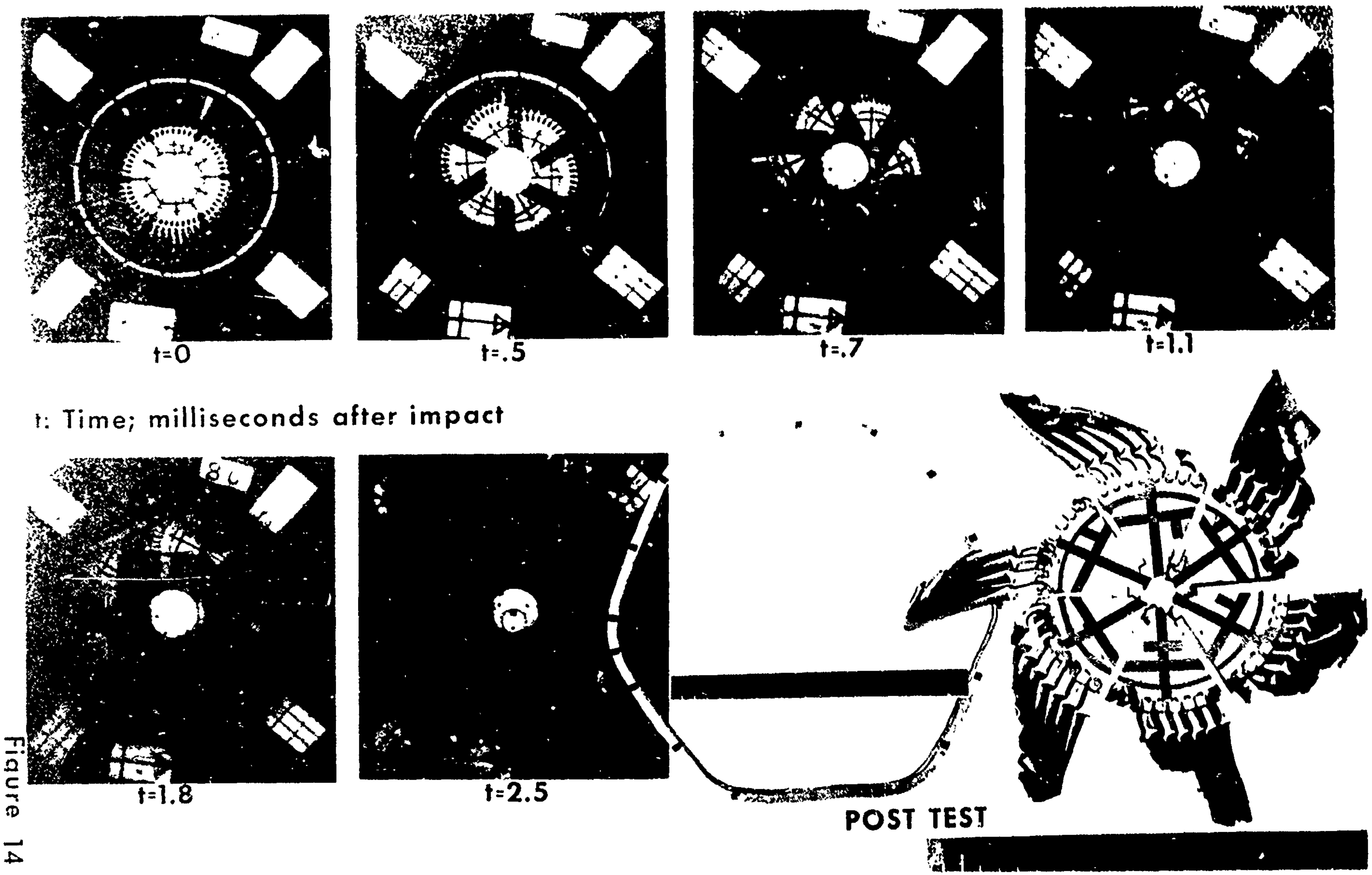

Figure 14

EXPERIMENT 120 -

2 FRAGMENT ROTOR BURST INTO RIGIDLY ATTACHED STEEL HALF RINGS

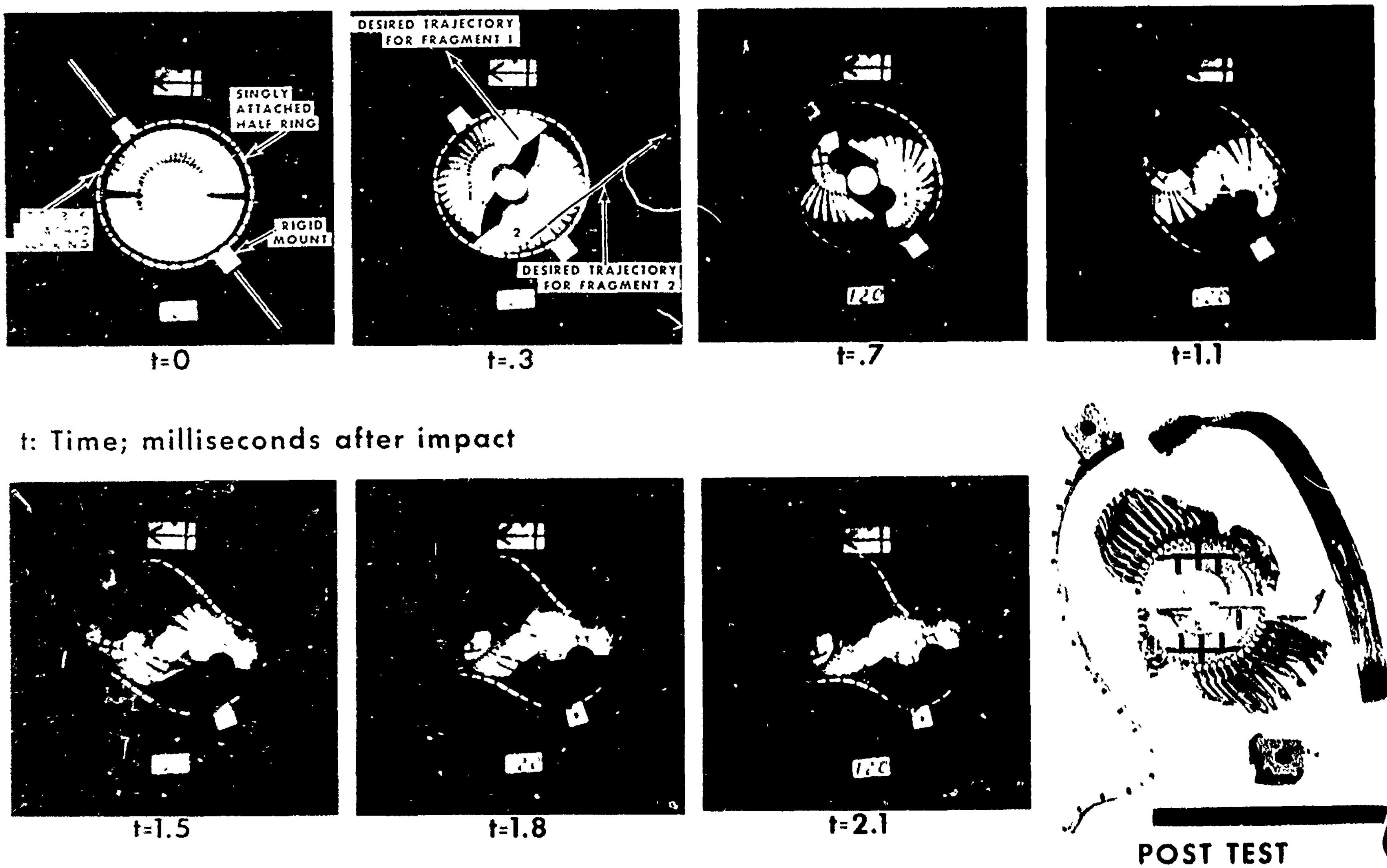

Figure 15

EXPERIMENT 123 -

2 FRAGMENT ROTOR BURST INTO FREELY SUPPORTED STEEL HALF RINGS

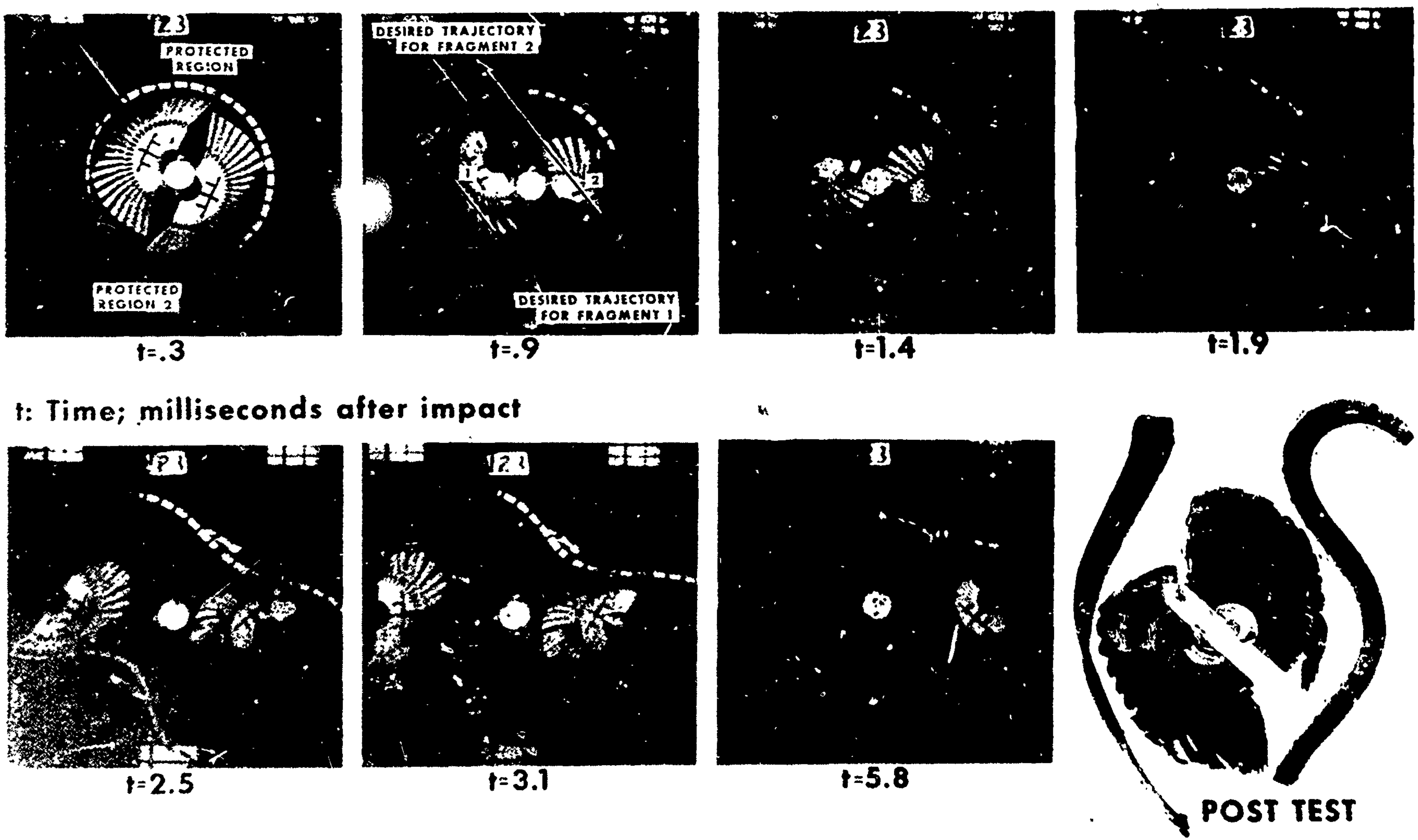

Figure 16

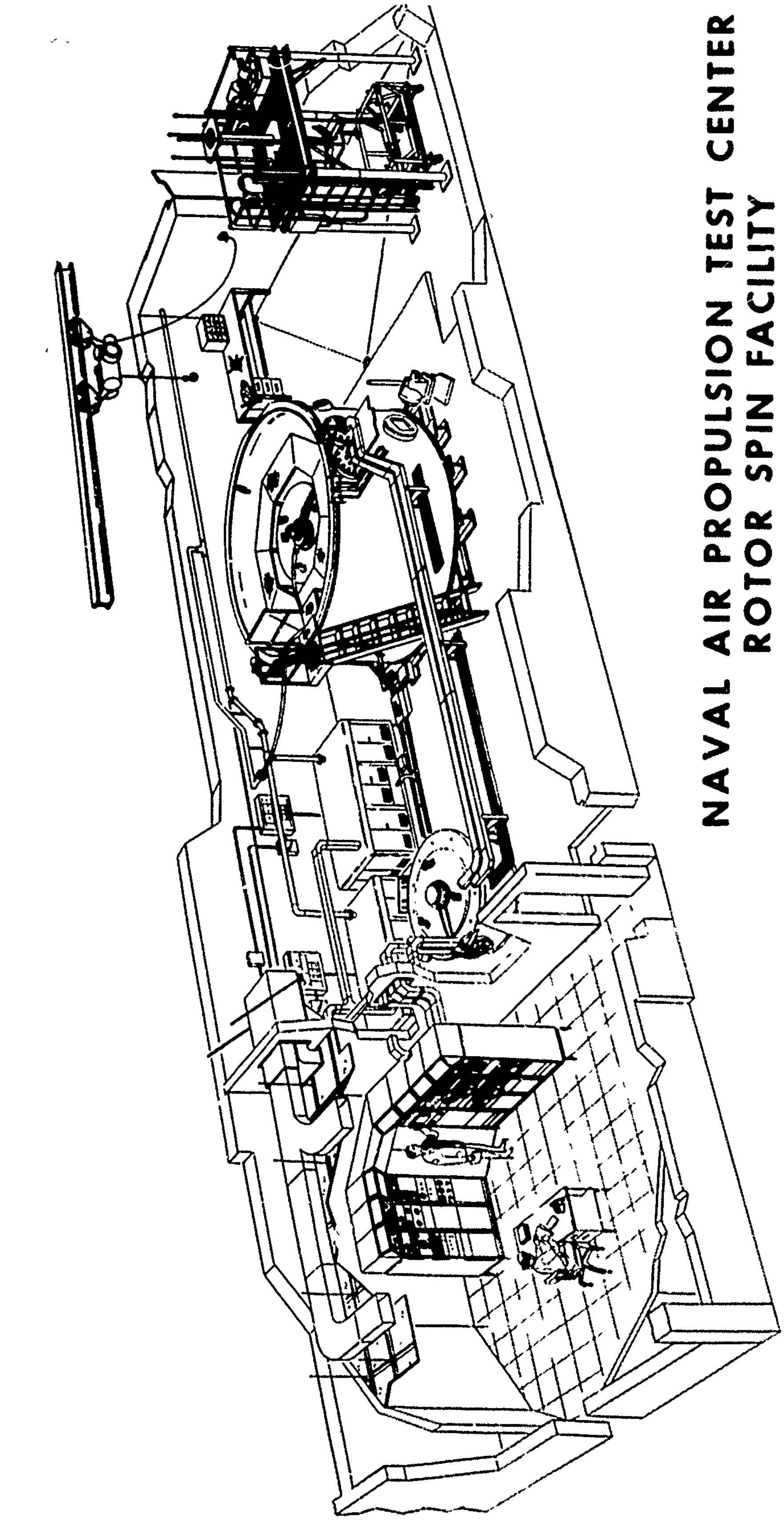

NAVAL AIR PROPULSION TEST CENTER
ROTOR SPIN FACILITY

Figure 17

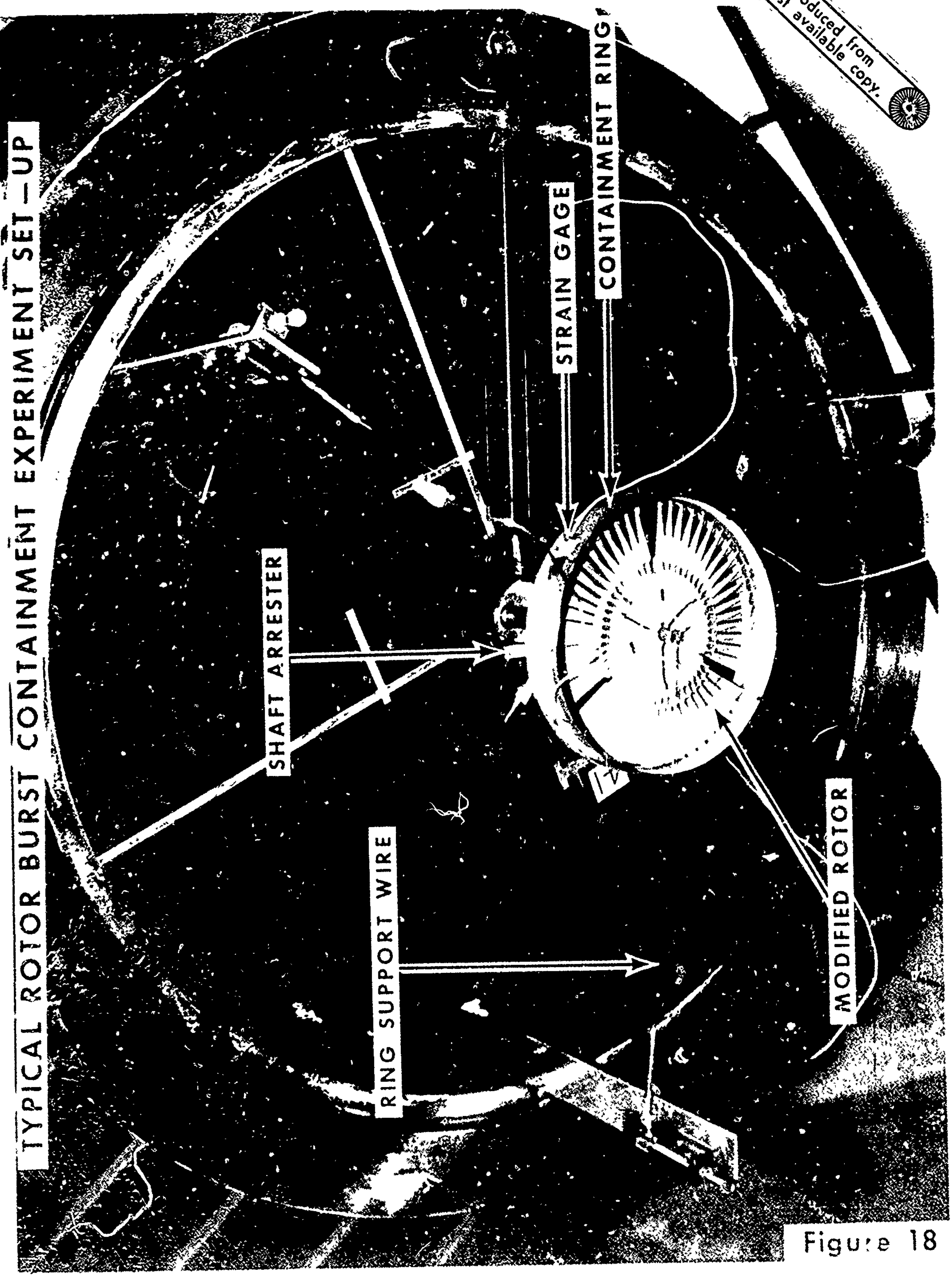
TYPICAL ROTOR BURST CONTAINMENT EXPERIMENT SET—UP
STRAIN GAGE
CONTAINMENT RING
SHAFT ARRESTER
RING SUPPORT WIRE
MODIFIED ROTOR

Figure 18

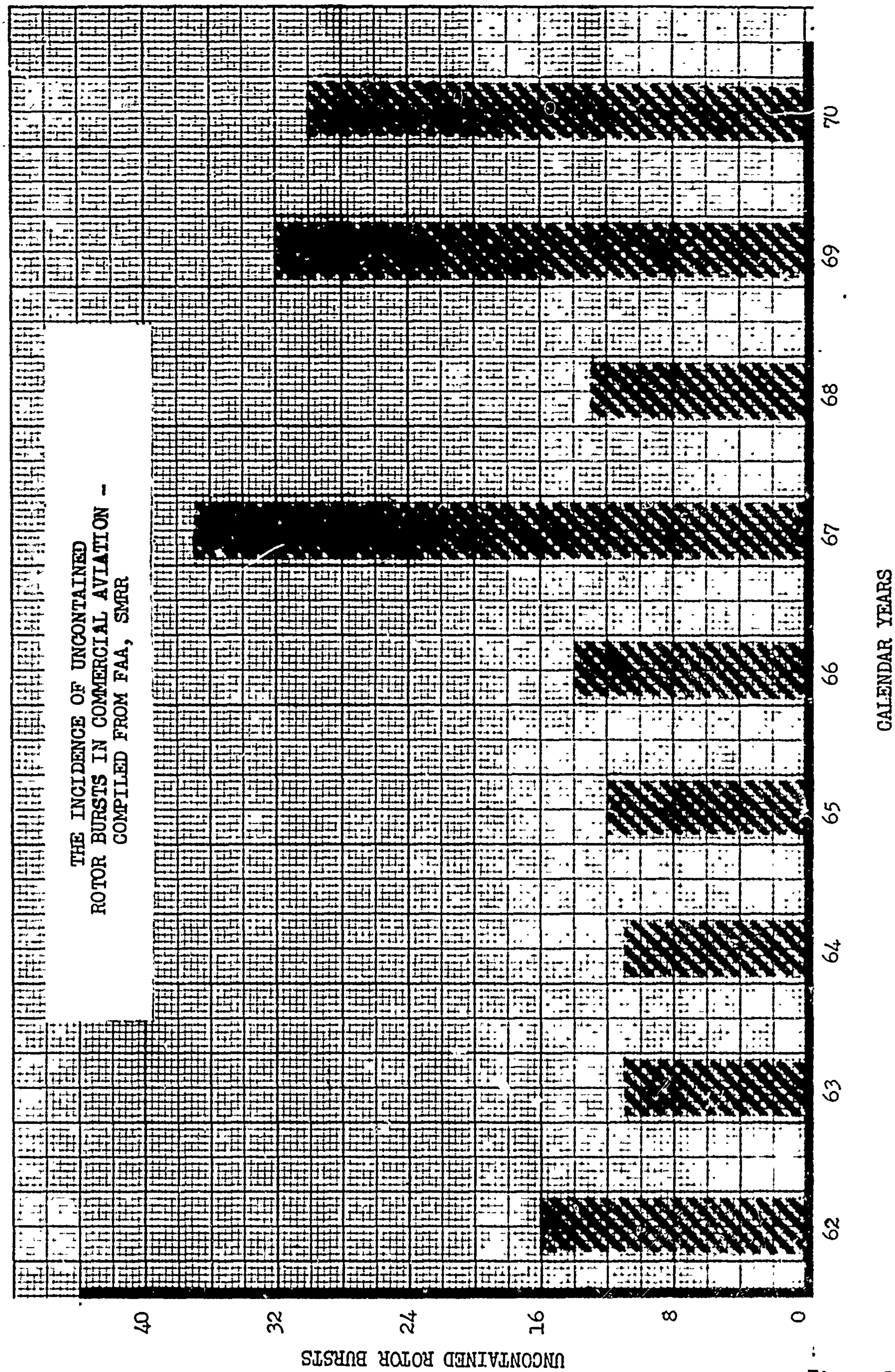
THE INCIDENCE OF UNCONTAINED
ROTOR BURSTS IN COMMERCIAL AVIATION -
COMPILED FROM FAA, SMRR
UNCONTAINED ROTOR BURSTS
0
8
16
24
32
40
CALENDAR YEARS
62
63
64
65
66
67
68
69
70

Figure 19

APPENDIX A

PROGRAM FOR THE DEVELOPMENT OF ROTOR BURST FRAGMENT CONTAINMENT RING DESIGN CRITERIA

1. A program of systematic rotor burst containment experimentation has been developed and is being conducted at the Naval Air Propulsion Test Center (NAPTC). This program is structured to develop criteria for the design of optimum weight turbomachine rotor fragment containment rings. The design criteria are generated by experimentally establishing the functional relationship between a specific energy variable that provides a measure of ring containment capability and several select variables which characterize those physical aspects of the containment rings and rotor fragments that significantly influence the fragment containment process. The specific energy variable (the dependent variable) involves the rotor fragment energy and the weight of ring required to contain this fragment energy. It is termed the Specific Contained Fragment Energy (SCFE) and is derived by dividing the rotor energy at failure by the ring weight.

The four ring and rotor variables, which are being varied to determine how they affect the containment potential or characteristic of the ring (as measured by the SCFE), are:

a. The ring inner diameter: Two diameters, one approximately twice as large as the other, are being used for experimentation with rotors having correspondingly larger and smaller tip diameters.

b. The ring axial length: Three axial lengths are being used corresponding to 1/2, 1 and 2 times the axial lengths of the large and small diameter rotors.

c. The number of rotor fragments generated at failure: The rotors are modified to fail at their respective design speeds and produce pie-sector shaped fragments having included angles of 60°, 90°, 120° and 180°. These are designated as 6, 4, 3 and 2-fragment rotor failures, respectively.

d. The ring radial thickness or outer diameter: The ring thickness is being varied until fragment containment is achieved for all combinations of ring (rotor) diameter, ring axial length, and the number of rotor fragments.

2. Other factors which will have considerable effect on the rotor fragment containment process are:

a. The mechanical properties of the rotor and ring materials.

b. The fragment velocities.

c. The rotor-to-ring radial clearance.

d. The rotor-tip-to-hub diameter ratio.

All of these factors will in some way influence the magnitude and orientation of the forces that are developed and the deformations and displacements that are sustained by the ring and rotor during containment interaction. However, with the exception of the factor noted in paragraph 2a, the variability of the remaining factors is constrained within narrow limits by the dictates of good aerodynamic, thermodynamic, and structural rotor design. For all practical purposes then, these factors are essentially constant from one turbomachine to another; therefore, there is no need to vary them in the experiments being conducted, and the results of these experiments will be representative of rotor containment characteristics from a wide variety of axial flow turbomachines.

3. Although the mechanical properties of the materials used to make the containment rings can vary widely and are considered to be important factors in fragment containment design, the ring material being used for the experiments currently being conducted are purposely the same from one experiment to the other. Later, when the effects of the other variables have been established, the influence that the ring material mechanical properties has on the fragment containment process will be studied and incorporated into the main body of information that represents the criteria for containment ring design.

4. To summarize:

a. The program consists of a series of rotor burst containment experiments in which rotors of two different diameters are modified to burst at their respective design speeds into various numbers (2, 3, 4 and 6) of pie-sector fragments. These fragments will impact rings made from 4130 cast steel that are freely supported and concentrically encircle the rotors at a radial clearance of 0.5 inches. The ring axial lengths are varied in three discrete steps of 1/2, 1, and 2 times the axial length of the rotors and their radial thickness are varied until fragment containment is achieved.

b. To generate the data needed to formulate the functional relationships that have been discussed and which, in concept, are shown graphically in Figure 1, rotor burst containment experiments are being conducted according to the test matrices shown in Figure 2. The use of these functional relationship curves to design an optimum weight steel ring for a particular rotor application can be best described by an example of their general use:

(1) Only two things must be known about the rotor prior to the design analysis:

(a) The kinetic energy (KE_R) content at burst.

(b) The size including tip diameter, axial length, and hub-to-tip diameter ratio.

The functional relationships between the SCFE, the number of fragments and rotor diameter with the ratio of the ring axial length to the rotor axial length as the parameter, provide an indication of what the worst combination of burst conditions would be for the size rotor being considered: i.e., the lowest SCFE. Once the value of SCFE is obtained from the curves, it is divided into the total energy of the rotor at burst. The result of this division is the optimum weight of steel ring required to contain the rotor fragments.

$$(1) \quad W_t = \frac{KE_R}{SCFE}$$

This weight is used in equation (2) to calculate the radial ring thickness required to effect containment.

$$(2) \quad T = \left[r_i^2 + \frac{W_t}{\rho \pi L_A} \right]^{\frac{1}{2}} - r_i$$

Where:

T = ring radial thickness

r_i = ring inner radius, which for practical purposes, equals the rotor radius: Rotor-to-casing operational clearances and considerations of minimum ring weight (the weight of a ring is directly proportional to the square of its inner radius) dictate that the ring and rotor radius be as equivalent as possible.

KE_R = rotor energy at burst

SCFE = Specific Contained Fragment Energy factor: The value taken from the curve in Figure 1 for the size rotor being considered: the number of rotor fragments that result in the most adverse containment condition (the lowest SCFE value in the SCFE-NF plane); and the optimum ring-to-rotor axial length ratio $\left(\frac{LRG}{LRT}\right)$ which is represented by the highest contour in Figure 1.

This general development of the data illustrates how the experimental results can be used by designers to establish the weight and size of rings needed to contain rotor burst fragments.

SCFE Specific Contained Fragment Energy
RD - Ring (Rotor) Diameter
NF - Number of Fragments
LRG Ring Axial Length
LRT Rotor Axial Length

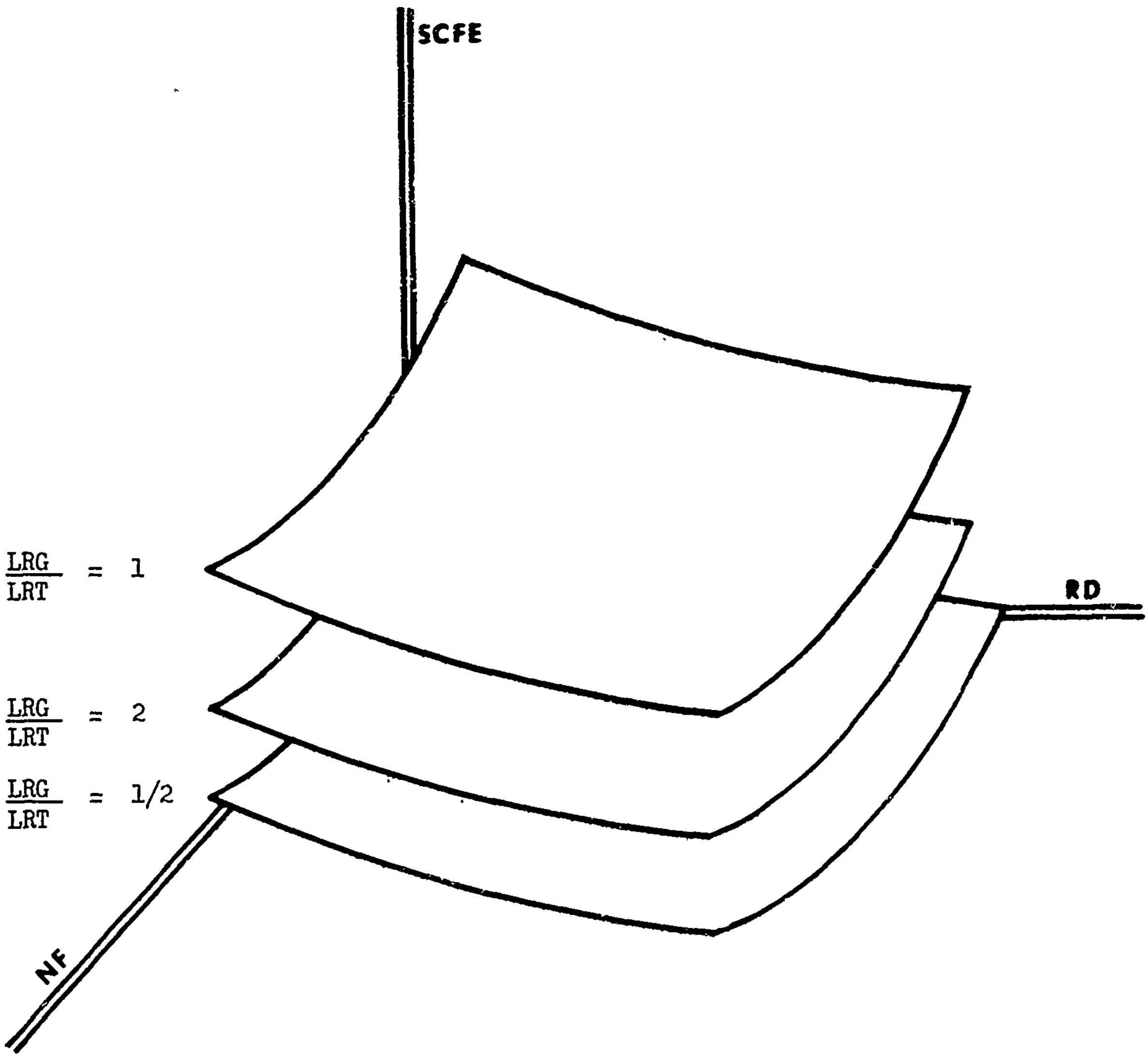

APPENDIX A

ROTOR BURST CONTAINMENT, FUNCTIONAL RELATIONSHIP, OR DESIGN CURVES (CONCEPTUAL)

Figure 1

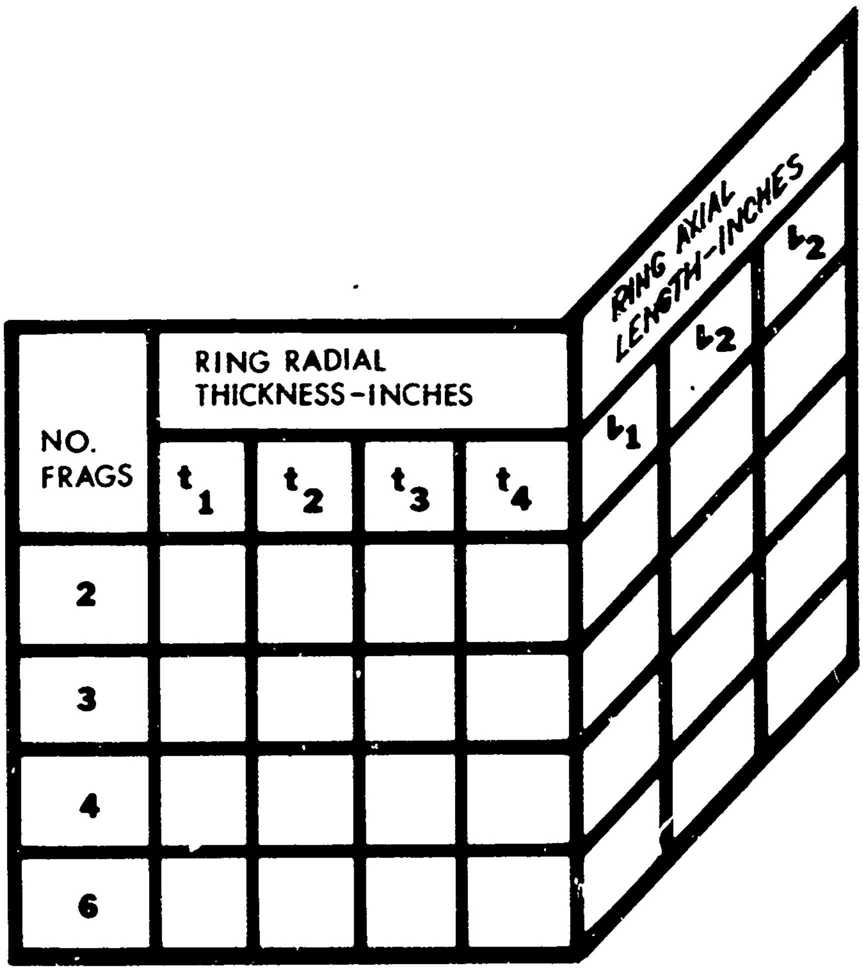

APPENDIX A

EXPERIMENTAL MATRICES FOR LARGE AND SMALL ROTOR BURST BURST CONTAINMENT DESIGN CRITERIA DEVELOPMENT PROGRAM

Figure 2

ACKNOWLEDGEMENTS

The author would like to credit and thank the following individuals for their excellent contributions to Phases VI and VII of the Rotor Burst Protection Program.

- Patrick T. Chiarito, NASA Lewis Research Center, for overall direction and management of the Program.

- Doctors John W. Leech and Emmett A. Witmer, Massachusetts Institute of Technology, for conceptual and analytical support and consultation.